Arabidopsis inositol polyphosphate kinases regulate COP9 signalosome deneddylase functions in phosphate-homeostasis

Yashika Walia[1], Mritunjay Kasera[1], Kishor D Ingole[1,2], Swaroop Peddiraju[1], Abhisha Roy[1], Debabrata Laha[3], Gabriel Schaaf[4], and Saikat Bhattacharjee[1*]

[1]Laboratory of Signal Transduction and Plant Resistance, UNESCO-Regional Centre for Biotechnology (RCB), NCR Biotech Science Cluster, 3rd Milestone, Faridabad-Gurgaon Expressway, Faridabad- 121 001, Haryana, India.

[2]Kalinga Institute of Industrial Technology (KIIT) University, Bhubaneswar- 751 024, Odisha, India.

[3]Department of Biochemistry, Indian Institute of Science, Bengaluru, Karnataka- 560 012, India.

[4]Department of Plant Nutrition, Institute of Crop Science and Resource Conservation, Rheinische Friedrich-Wilhelms-Universität Bonn, 53115 Bonn, Germany.

*Corresponding author:

Saikat Bhattacharjee

saikat@rcb.res.in

Tel: (+91) 0129-2848837

ORCID ID

Saikat Bhattacharjee https://orcid.org/0000-0003-1369-7700

Gabriel Schaaf https://orcid.org/0000-0001-9022-4515

Yashika Walia https://orcid.org/0000-0001-8122-8661

Mritunjay Kasera https://orcid.org/0000-0002-1110-3502

Kishor D Ingole https://orcid.org/0000-0003-1946-6639

Swaroop Peddiraju https://orcid.org/0000-0001-5290-7067

Abhisha Roy https://orcid.org/0000-0002-3431-0811

Debabrata Laha https://orcid.org/0000-0002-7823-5489

Author Contributions

Y.W. and S.B. conceived and designed the research. D.L. and G.S. generated transgenic line used here. Y.W. and S.B. performed most of the experiments. Y.W., M.K., K.D.I, S.P., and A.R. conducted and analyzed gene/protein expression changes. Y.W. and S.B. wrote the manuscript.

Competing interest statement

The authors declare no conflict of interest for this study.

Keywords

Inositol polyphosphates, COP9 signalosome, CSN5, IP5K, IP6K1, IPK1, ITPK1

Abstract

Targeted protein degradation is essential for physiological development and adaptation to stress. Mammalian INOSITOL PENTAKISPHOSPHATE 2-KINASE (IP5K) and INOSITOL HEXAKISPHOSPHATE KINASE 1 (IP6K1) pair generates inositol polyphosphates (InsPs) to modulate association/dissociation equilibrium of Cullin RING Ubiquitin E3 ligases (CRLs) on the COP9 signalosome (CSN) platform. Deneddylase activity of the CSN5 subunit protects cullins from self-ubiquitination ensuring their functional continuity. In plants, similar regulations by InsP-kinases are not known. Here, we show conserved interactions of *Arabidopsis thaliana* INOSITOL PENTAKISPHOSPHATE 2-KINASE 1 (IPK1) and INOSITOL 1,3,4-TRISPHOSPHATE 5/6-KINASE 1 (ITPK1), counterparts of the above mammalian InsP-kinase pair, with selective CSN subunits. In *ipk1* or *itpk1* mutants, deneddylation deficiencies not only cause increased neddylated Cullin1 ($CUL1^{Nedd8}$) pools more prone to degradation but also impair CSN5 entry/exit shuttles on the CSN holo-complex. Constitutive phosphate-starvation response (PSR), previously known for these mutants are suppressed by pharmacological inhibition of neddylation thus linking CSN-CRL functions to phosphate (Pi)-sensing. Similarly, in wild-type plants exposed to compounds that impair CSN5 deneddylase function affects its dynamics and mimic PSR properties of the mutants. We further show that under Pi-deprivation more CSN5 retentions on the CSN holo-complex and the resulting enhanced $CUL1^{Nedd8}$ pools is essential for induction of downstream Pi-starvation inducible (PSI) genes. Overall, with our data we present InsP-kinase involvements in maintenance of Pi-homeostasis in plants via CRL-CSN(5) functional synergism.

Significance

Neddylation modifications on Culling-RING E3 ligases (CRLs) while essential for their role in proteostasis, also threaten their own stability. Selective inositol polyphosphates (InsPs) aid

the constitutive photomorphogenesis 9 signalosome (CSN) functions in protecting, deneddylating, and facilitating CRL recycling. Here we demonstrate that plant mutants deficient in these InsPs have disturbed CSN subunit partitioning, are deficient in deneddylase activity, and hyperaccumulate neddylated cullins that lead to constitutive phosphate-starvation response (PSR). Inhibition of CSN functions/consequences mirror the InsP mutant properties indicating pivotal involvement of CSN in phosphate homeostasis. These raises promising possibilities of targeted intervention on CSN functions for nutritional benefit of plants.

69 **Introduction:**

70 The versatile functions of inositol polyphosphates (InsPs) in cellular processes of all eukaryotes
71 are owed to its propensity for differential degree of phosphorylation catalyzed by relatively
72 conserved set of InsP-kinases (Stevenson-Paulik *et al*., 2005; Monserrate and York, 2010;
73 Shears and Wang, 2019). In plants, selective InsPs have been linked to phytohormone
74 networks, inorganic phosphate (Pi)-homeostasis, mRNA export, (a)biotic stress responses,
75 among others (Stevenson-Paulik *et al*., 2005; Murphy *et al*., 2008; Gillaspy, 2013; Lee *et al*.,
76 2015; Williams *et al*., 2015; Jia *et al*., 2019). With all six-hydroxyl group of the *myo*-inositol
77 ring phosphorylated, $InsP_6$ (myo-inositol-1,2,3,4,5,6-hexakisphosphate or phytic acid),
78 produced by INOSITOL PENTAKISPHSPHATE 2-KINASE 1 (IPK1) is sequentially (pyro)-
79 phosphorylated by INOSITOL 1,3,4-TRISPHOSPHATE 5/6-KINASES (ITPK1/2) and then
80 by DIPHOSPHOINOSITOL PENTAKISPHOSPHATE KINASES (VIH1/2) to generate
81 energy-rich phosphoanhydride bond-containing inositol pyrophosphates $InsP_7$ and $InsP_8$,
82 respectively (Desai *et al*., 2014; Laha *et al*., 2015; Adepoju *et al*., 2019; Laha *et al*., 2019).
83 Though *bona fide* receptors of plant InsPs remain unidentified, their co-factor functions are
84 being increasingly elaborated (Shears *et al*., 2012; Williams *et al*., 2015). While $InsP_6$, or more
85 recently speculated $InsP_7$, promotes auxin-dependent degradation of AUX/IAA repressors,
86 $InsP_8$ targets JASMONATE ZIM-DOMAIN (JAZ) repressors in a jasmonic acid (JA)-
87 dependent manner (Tan *et al*., 2007; Sheard *et al*., 2010; Laha *et al*., 2015; Laha *et al*., 2020).
88 Interestingly, the cognate substrate receptors TRANSPORT INHIBITOR RESPONSE 1
89 (TIR1) or CORONATINE INSENSITIVE 1 (COI1) belong to F-box family proteins and are
90 components of typical SCF (ASK1/SKP1-Cullin-F-Box; SCF^{TIR1} or SCF^{COI1})-type E3
91 ubiquitin ligases (Tan *et al*., 2007; Sheard *et al*., 2010). The *ipk1* or *itpk1* mutants with reduced
92 $InsP_7$ or *vih2* plants with reduced $InsP_8$, are auxin- or JA-insensitive, respectively (Laha *et al*.,
93 2015; Laha *et al*., 2020).

94 InsPs have also been recently implicated as sensor of phosphate (Pi)-status in plants (Kuo *et*
95 *al*., 2018; Dong *et al*., 2019; Ried *et al*., 2019; Zhu *et al*., 2019). Necessity of phosphates in
96 central dogma processes, protein modifications, and most importantly as indicators of
97 adenylate currencies risk detrimental consequences when cellular Pi levels are low (Szijgyarto
98 *et al*., 2011; Wundenberg and Mayr, 2012). Under a low Pi-availability from soil, a highly
99 organized adaptive cascade of events collectively termed as PSR is activated and includes
100 increased remobilization of Pi from root to shoot, harnessing of organellar Pi-storage reserves,
101 accompanied by upregulated expression of PSI genes for Pi-transporters (*PHT*s), phosphatases
102 (*PAP*s), and several micro- (*MIR399*) or non-coding RNAs (*IPS1*) (Puga *et al*., 2014; Ham *et*
103 *al*., 2018). In Arabidopsis, PSR-associated transcriptional changes are majorly orchestrated by
104 the MYB-transcription factors PHOSPHATE STARVATION RESPONSE 1 (PHR1) and its
105 closest homolog PHR1-LIKE (PHL1) (Bustos *et al*., 2010). These transcription factors bind to
106 partially conserved sequences (P1BS elements) present on PSI gene promoters to activate their
107 transcriptions (Rubio *et al*., 2001). A *phr1 phl1* double mutant is deficient in PSI-gene
108 expressions both basally as well as upon exposure to Pi-deplete conditions (Kuo *et al*., 2014).

109 A class of stand-alone SPX (SYG1/Pho81/XPR1)-domain containing proteins SPX1/2 act as
110 negative regulators of PHR1/PHL1 functions in maintaining phosphate balances in a cell.
111 Following the first report that SPX domains can bind specific InsPs it was subsequently
112 demonstrated that under Pi-replete conditions, SPX1 requires $InsP_8$ co-factor to bind PHR1,
113 sequester it away from the nucleus, and suppress its activity (Wild *et al*., 2016; Jung *et al*.,
114 2018; Dong *et al*., 2019; Zhu *et al*., 2019). When starved for Pi, intracellular $InsP_8$ levels reduce
115 because of the phosphatase activity of VIH2 relieving SPX1-tethered inhibitions on PHR1,
116 thus allowing successful transduction of PSR (Dong *et al*., 2019). In $InsP_8$-deficient *ipk1-1*,
117 *itpk1-2*, or *vih1 vih2* and in the *spx* mutants liberated PHR1 causes constitutive activation of
118 PSI-gene expressions even under Pi-sufficient conditions accumulating high endogenous Pi

levels (Kuo *et al*., 2014; Puga *et al*., 2014; Dong *et al*., 2019; Zhu *et al*., 2019). Decreased $InsP_8$ levels that occur upon Pi-starvation also promotes ubiquitinylation of at least two SPX proteins (Lv *et al*., 2014; Zhong *et al*., 2018; Osorio *et al*., 2019). Recent identification of E3 ubiquitin ligases that target rice SPX4 upon Pi-starvation (Ruan *et al*., 2019) taken together with specific InsP-requirement in determination of fate of hormonal repressors, $InsP_7$/$InsP_8$ clearly are also biochemical regulators of stimulus-dependent substrate stabilities.

In a typical eukaryotic cell, ~20% of targeted protein degradations are mediated by Cullin RING ubiquitin ligases (CRLs), the largest member among the E3 ubiquitin ligase family (Soucy *et al*., 2009; Yi Sun, 2020). A modular CRL contains a Cullin (CUL) scaffold (CUL1-4 in Arabidopsis), an E2-interacting RING-type Rbx/Roc protein, CUL member-specified substrate adaptor and a ubiquitination target-specified substrate receptor. CRLs require covalent modification of a Nedd8 moiety on CULs (a process termed as neddylation) for function (Yi Sun, 2020). Neddylations improve CRL efficiencies in complex formation with the ubiquitin E2 enzyme for subsequent degradation of targeted substrates. In absence of cognate substrates self-ubiquitinylation-vulnerable CRLs are protected on Constitutive photomorphogenesis 9 signalosome (CSN), an evolutionarily conserved eight-subunit (CSN1-8) macromolecular complex (Chamovitz and Segal, 2001; Dubiel *et al*., 2015). The CSN5 subunit in this holo-complex contains an MPN+/JAMM metalloprotease motif that catalytically removes Nedd8 (deneddylation) from CULs (Cope *et al*., 2002) causing CRL disassembly and promoting newer associations with substrate receptors and adaptors required for continuum of its functions. Interaction changes between CRL-CSN affect cellular ratio of neddylated CUL: unneddylated CUL (CUL^{Nedd8}:CUL) (Scherer *et al*., 2016). Biochemical modes of a CSN operation including its dynamic rearrangements upon CRL binding have been gradually unraveled at structural and functional levels (Enchev *et al*., 2012; Lingaraju *et al*., 2014; Dubiel *et al*., 2015). From these studies, it is evident that optimal CRL activity

144 necessitates regulated neddylation/deneddylation cycles of CULs. Neddylated CRLs are
145 captured on the CSN holo-complex only in deneddylation-deficient *csn* mutants inferring that
146 deneddylation-dependent disassembly is very rapid (Enchev *et al*., 2012). The 'CSN paradox'
147 (Dubiel, 2009), an apparent contradiction between genetic requirement of a CRL for CSN-
148 protection at the cost of its deneddylation-dependent inactivation is now better understood at a
149 molecular level. Recent breakthroughs show that highly locale-specific coordinated activities
150 of mammalian IP5K with IP6K1, functional homologs of Arabidopsis IPK1 and ITPK1,
151 provide $InsP_6$ to strengthen and $InsP_7$ to loosen CRL-CSN associations (Rao *et al*., 2014;
152 Scherer *et al*., 2016; Lin *et al*., 2020). Through intricate orchestrations, a CRL tether-promoting
153 $InsP_6$ is converted to the liberator $InsP_7$ by an inert IP6K1 that gets activated at CSN only upon
154 a stimulus. This synchronization ensures functional demands of CRLs meet the response
155 requirements proportionately without a compromise on its own stabilities. With reported
156 interactions between Arabidopsis ITPK1 and CSN1 (Qin *et al*., 2005), direct implication of
157 (any) InsP-kinase on CSN-activities from a plant system has not been forthcoming.

158 Here we show that Arabidopsis IPK1-ITPK1 pair retains conserved CSN interactions and
159 modulate CUL1 deneddylation efficiencies impacting association/dissociation kinetics of
160 CSN5 on the CSN holo-complex. Unlike noted in animal cells, CRL-CSN associations remain
161 mostly unaffected in *ipk1* or *itpk1* mutants. Nevertheless, enhanced level of CUL^{Nedd8} result in
162 constitutive PSR in these mutants. Further, we reveal that Pi-deprivation in wild-type plants is
163 associated with CSN(5) perturbations and increased CUL1 neddylation that precedes
164 PHR1/PHL1 role in inducing PSI gene expressions. Mutational or pharmacological inhibitions
165 of CSN5 result in constitutive PSR even under sufficient Pi-availability. However, when
166 actually Pi-starved, PSR responses in these plants or in the *ipk1* or *itpk1* mutants are suppressed
167 indicating that equilibrium shifts of CSN5 deneddylase activity rather than its complete
168 inhibition is essential to execute PSR. Our investigations overall reveal activities of plant IPK1-

169 ITPK1 pair in regulating CSN dynamics, its consequences on CRLs functions and requirement
170 in maintaining Pi-homeostasis or responding to its deficiencies.

171

172 **Results**

173 **Arabidopsis IPK1 and ITPK1 interact with CSN holo-complex subunits.**

174 Mammalian IP5K co-precipitates with CSN2/5 whereas IP6K1 interacts with CSN1/2 (Rao *et*
175 *al*., 2014; Scherer *et al*., 2016). Arabidopsis ITPK1 associates with CSN1 (Qin *et al*., 2005).
176 Interactions of Arabidopsis IPK1 with CSN subunits have not been investigated earlier. We
177 immuno-enriched Myc-IPK1 or ITPK1-GFP from *ipk1-1*:*Myc-IPK1* and *itpk1-2*:*ITPK1-GFP*
178 transgenic lines, respectively and probed for the presence of selective CSN subunits, CUL1 or
179 the substrate adaptor ASK1. These transgenic lines restore high endogenous Pi and elevated
180 PSI gene *SPX1* expressions to wild-type (Col-0) levels implicating the functionality of the
181 corresponding fusion proteins (Laha *et al*., 2020) (Supplemental Figure 1). In
182 immunoprecipitation assays, CSN1/2/4/5, CUL1 and ASK1 co-purified with IPK1, whereas
183 ITPK1 enrichments detected CSN1/2 and ASK1 (Figure 1A). Through Bimolecular
184 Fluorescence Complementation (BiFC) assays, IPK1 or ITPK1 association with CSN1 and
185 CSN2 are detected as nucleocytoplasmic complexes similar to localization of the individual
186 proteins (Adepoju *et al*., 2019) (Figure 1B). A negative control β-Glucuronidase (GUS) protein
187 does not interact with IPK1, ITPK1 or CSN1/2 (Supplemental Figure 2). These data suggest
188 that likewise to animals, CSN associations of IPK1 and ITPK1 are conserved in Arabidopsis.
189 Although biochemically coupled by substrate-product relationship, interaction between IPK1
190 and ITPK1 has not been demonstrated *in planta*. To this end, BiFC detects IPK1-ITPK1
191 complexes at nucleocytoplasmic locales (Figure 1B). Further, we performed co-
192 immunoprecipitation assays via transient co-expression of Myc-IPK1 and GFP-ITPK1 in

193 *Nicotiana benthamiana* leaves. Enrichment of GFP-ITPK1 with anti-GFP affinity beads co-
194 elutes Myc-IPK1 indicating their associations *in vivo* (Figure 1C). Overall, our results
195 recapitulate IPK1 and ITPK1 interactions with CSN and with each other.

196 To determine cellular proportions of IPK1 or ITPK1 that associate with the CSN holo-complex,
197 we subjected Col-0, *ipk1-1*:*Myc-IPK1* and *itpk1-2*:*ITPK1-GFP* extracts to size-exclusion
198 chromatography followed by immunoblots for representative CSN subunits, Myc-IPK1 or
199 ITPK1-GFP. The elution patterns of molecular weight standards and selective CSN subunits
200 with demarcation of CSN holo-complex fractions, as noted in earlier reports are shown
201 (Gusmaroli *et al*., 2004; Dohmann *et al*., 2005) (Figure 2A). CSN1, exclusively associates with
202 the CSN holo-complex and elutes accordingly in higher molecular weight pools (>600-400
203 kDa). CSN4 and CSN5 fractionates both as a part of CSN holo-complex as well as in lower
204 molecular weight pools (monomers, 100-50 kDa). Partitioning profiles of CSN5 and CSN4 are
205 comparable between Col-0, *ipk1-1*:*Myc-IPK1* and *itpk1-2*:*ITPK1-GFP* (Figure 2B;
206 Supplemental Figure S3A). Remarkably, neither Myc-IPK1 nor ITPK1-GFP proteins are
207 detected in fractions corresponding to the CSN holo-complex implying that their associations
208 are either transient or represent only marginal proportions of these proteins (Figure 2A). Co-
209 elution of Myc-IPK1 and ITPK1-GFP in overlapping fractions is likely indicative of their *in*
210 *vivo* associations we noted earlier.

211 **CSN5 deneddylase deficiencies cause enhanced CUL1^{Nedd8} pools in *ipk1* or *itpk1* plants.**

212 Depletion of IP5K or IP6K1 reduces CRL-CSN associations in mammalian systems (Rao *et*
213 *al*., 2014; Lin *et al*., 2020). To examine whether in *ipk1-1* or *itpk1-2* lower CUL1 pools co-
214 fractionate with the CSN holo-complex, we immuno-enriched CUL1 from Col-0, *ipk1-1* or
215 *itpk1-2* extracts and probed for the presence of CSN1/2. Although slightly lower CUL1 was
216 immunoprecipitated from *ipk1-1* or *itpk1-2* than Col-0, nonetheless proportionately similar

217 amounts of CSN1/2 as in Col-0 co-eluted suggesting that CRL-CSN associations are likely not
218 perturbed in these mutants (Figure 2C). Surprisingly, when we compared elution profiles,
219 CSN5 but not CSN4 in *ipk1-1* or *itpk1-2* extracts showed increased presence in CSN holo-
220 complex fractions with marked decrease in monomeric elutions, relative to Col-0 (Figure 2B).
221 Total CSN5 levels however remained comparable between all plants.

222 Resident CSN5 performs the deneddylase role in a CSN holo-complex (Cope *et al*., 2002).
223 With changed partitioning of CSN5 noted in *ipk1-1* or *itpk1-2* we tested whether deneddylation
224 efficiencies on CULs are impacted. In mammalian system depleting IP5K or IP6K1 causes
225 strong increments in CUL^{Nedd8} levels (Rao *et al*., 2014; Scherer *et al*., 2016). Remarkably, in
226 *ipk1-1* or *itpk1-2* lysates, enhanced $CUL1^{Nedd8}$ levels relative to Col-0 are strikingly prominent
227 (Figure 2D). These increases are specific to *ipk1-1* or *itpk1-2* and extracts from *ipk2β-1* with
228 low $InsP_6$ levels as *ipk1-1* (Stevenson-Paulik *et al*., 2005), *vih2-4* plants with elevated $InsP_7$
229 (Laha *et al*., 2015), or *itpk4-1* with low $InsP_6$ and $InsP_7$ levels (Kuo *et al*., 2018) do not show
230 elevated $CUL1^{Nedd8}$ pools (Supplemental Figure S3B). In the respective complemented lines of
231 *ipk1-1* or *itpk1-2*, CUL^{Nedd8}:CUL ratios are restored comparable to Col-0 (Figure 2D).

232 Global ubiquitinylation is enhanced due to loss of mammalian IP6K1 (Rao *et al*., 2014). As a
233 possible consequence to increased CUL^{Nedd8} levels, we tested relative levels of ubiquitinylation
234 in Col-0, *ipk1-1*, or *itpk1-2* extracts. Clear increase in global ubiquitin-conjugates in
235 appearance of a smear when probed with anti-ubiquitin antibodies is detected in the mutant
236 plants than Col-0 (Figure 2D). In complemented lines, wild-type ubiquitinylation levels are
237 noted. Further, in-lysate deneddylation assay to determine deneddylase defects (Lin *et al*.,
238 2020) reveal decreased efficiencies of CUL1-deneddylation by endogenous CSN5
239 simultaneous with increased CUL1 turnover rates in *ipk1-1* or *itpk1-2* extracts (Figure 2E).
240 Decreased CUL1 stability likely accounts for the reduced immuno-enrichments from the
241 mutants observed earlier. Taken together, our results parallel animal studies demonstrating

242 impaired CSN5 deneddylase activity in *ipk1-1* or *itpk1-2* that leads to augmented $CUL1^{Nedd8}$
243 levels prone to increased turnover due to self-ubiquitinylation.

244 **Pi-starvation alters dynamics of CSN5 and its deneddylase efficiencies.**

245 Known consequences in *ipk1-1* and *itpk1-2* are auxin-insensitivity and constitutive PSR (Kuo
246 *et al*., 2014; Kuo *et al*., 2018; Laha *et al*., 2020; Riemer *et al*., 2020). Reduced $InsP_8$ in these
247 mutants likely disrupt SPX1-PHR1 interactions that lead to activation of PSI-genes (Ried *et*
248 *al*., 2019). MLN4924, a small molecule pharmacological inhibitor of CUL neddylation (Soucy
249 *et al*., 2009) is functional in Arabidopsis, inhibits degradation of CRL substrates and confers
250 auxin insensitivity (Hakenjos *et al*., 2011). To test whether increased PSI-gene expressions in
251 *ipk1-1* or *itpk1-2* are consequences of enhanced $CUL1^{Nedd8}$ levels via augmenting CRL
252 functions, we treated these mutants with MLN4924. Remarkably, upregulated expression of
253 PSI-genes such as *IPS1, SPX1,* or *PHT1;3* as well as high endogenous Pi levels in *ipk1-1* or
254 *itpk1-2* were suppressed by MLN4924-treatments (Figure 3A-B; Supplemental Figure 4A). On
255 Col-0 grown under Pi-sufficient conditions, MLN4924 treatments did not cause detectable
256 change in endogenous Pi-levels or *IPS1* expression (Figure 3A-B). Most surprisingly,
257 MLN4924 treatments on Col-0 suppressed the induction of *PHT1;3* or *IPS1* when subjected to
258 Pi-starvation implying that neddylation processes drive PSI-gene expressions (Figure 3C).

259 To test whether neddylation efficiencies of cullins are affected upon Pi-deprivation, extracts
260 from Col-0 grown under Pi-replete or Pi-deplete conditions were immunoblotted with anti-
261 CUL1 antibodies. Prominent increase in $CUL1^{Nedd8}$ levels, sensitive to MLN4924 inhibition,
262 was noted under Pi-starvation (Figure 3D). Interestingly, these enhancements were induced
263 even in the *phr1phl1* plants when subjected to Pi-deplete conditions implying that neddylation
264 readjustments are upstream of PHR1/PHL1 role in inducing PSI-gene expressions. Already
265 enhanced $CUL1^{Nedd8}$ levels in *ipk1-1* or *itpk1-2* remained unaffected under Pi-deplete

266 exposures (Supplemental Figure 4B). Taken together, our results identify CUL1
267 hyperneddylation as an early response to Pi-starvation essential for transducing downstream
268 signaling.

269 As tested earlier for *ipk1-1* or *itpk1-2*, to correlate increased $CUL1^{Nedd8}$ levels to decreased
270 CSN5 deneddylase activity, we performed in-lysate deneddylation assay on Pi-replete or
271 starved Col-0. Diminished CSN5 deneddylase activity was clearly apparent in Pi-deprived
272 Col-0 extracts (Figure 4A). In the same extracts CUL1 instabilities were not evident perhaps
273 reflecting tight regulations between its increased utilization and turnover rates. When profiled,
274 CSN5 elution patterns under Pi-deplete conditions were peculiarly similar to *ipk1-1* or *itpk1-2*
275 with more engagements on the CSN holo-complex and lower monomeric pools (Figure 4C).
276 Total CSN5 protein remained comparable between Pi-replete and Pi-deplete extracts. Profiles
277 of CSN1 remained unaltered by the Pi-changes (Supplemental Figure 4C). Resupplied
278 phosphate restored both CSN5 partitioning changes and increased $CUL1^{Nedd8}$ amounts to Pi-
279 replete pattern suggesting that observed changes were due to Pi-starvation (Figure 4B, C)
280 Curiously, unlike *ipk1-1* or *itpk1-2*, global ubiquitinylation was not enhanced upon Pi-
281 starvation although resupplying phosphate did cause a modest increase (Figure 4D). Together,
282 these results suggest intricate coordination between CSN-CRL activities to maintain specificity
283 in responding to reduced Pi-availability. Also, our data indicates that plants modulate CSN5
284 deneddylase activity and affect its dynamics during Pi-deprivation to induce PSI-gene
285 expressions, a phenomenon that is constitutive in *ipk1-1* or *itpk1-2*. In Pi-starved *ipk1-1:Myc-*
286 *IPK1* or *itpk1-2:ITPK1-GFP* plants, marked increase in ITPK1-GFP, but not very prominent
287 for Myc-IPK1 protein, was detected in comparison to non-starved extracts (Supplemental
288 Figure 4D). These at least are not due to increased transcriptions as reported earlier (Riemer et
289 al., 2020) and may instead be in accordance with increased stability the mammalian IP6K1
290 acquires when associated with an active CRLs (Rao *et al*., 2014).

291 **Functional inhibition of CSN5 phenocopy *ipk1* or *itpk1* responses.**

292 To determine whether PSI-gene expressions are globally affected by CSN functions, we mined
293 the available microarray data of differentially expressed transcripts in *csn* null mutants (*csn3*,
294 *csn4* and *csn5ab*) (Dohmann *et al*., 2008). Strong upregulation in expressions compared to
295 wild-type plants are especially noted in genes responsible for Pi-remobilization (*PAP1, PAP10,*
296 *PAP23, DFR, F3H*) and several Pi-transporters (*PHT3;2, PHT3;3, OCT1*) (Supplemental
297 Figure 5). Expressions of *PHR1* or *PHL1* remain unaffected in these mutants similar to *ipk1-1*
298 or *itpk1-2* (Kuo *et al*., 2014; Kuo *et al*., 2018). Also, neither *IPK1* nor *ITPK1* transcriptions are
299 changed in the *csn* mutants. Thus, CSN holo-complex dysfunctions affect several PSI-gene
300 expressions likely because of its deneddylation deficiencies. To explore CSN5 roles further,
301 we utilized the *csn5a-2* plants harboring a T-DNA insertion in the last exon of the *CSN5A*
302 isoform (*At1g22920*). Similar to *ipk1-1* or *itpk1-2*, *csn5a-2* extracts accumulate higher
303 $CUL1^{Nedd8}$ levels and display auxin-insensitivity (Gusmaroli *et al*., 2004; Dohmann *et al*.,
304 2005; Dohmann *et al*., 2008; Laha *et al*., 2020). Under Pi-replete growth, increased basal Pi-
305 levels accompanied by mild up-regulated expressions of *PHT1;3* or *SPX1* is detected in the
306 *csn5a-2* plants (Figure 5A-B). Also, primary root lengths of *csn5a-2* plants are slightly, but not
307 statistically shorter than Col-0 in this growth media (Supplemental Figure 6). These features
308 are very similar to *ipk1-1* or *itpk1-2* (Riemer *et al*., 2020). Growth under Pi-starvation led to
309 strong inhibition of primary root length in Col-0, while in *csn5a-2* (and in *ipk1-1* or *itpk1-2*)
310 plants these were prominently less. With exposure to Pi-deplete conditions, *csn5a-2* plants are
311 completely impaired in inducing *PHT1;3* or *SPX1* (Figure 5B). These results resemble PSI
312 gene induction deficiencies in *itpk1-2* when subjected to Pi-starvation (Riemer *et al*., 2020)
313 suggesting that CSN5 functions are necessary in maintenance of Pi-homeostasis and successful
314 transduction of PSR.

315 To directly relate CSN5 deneddylase role in Pi-homeostasis, we tested the effects of recently
316 reported CSN5 inhibitors Azaindole#6 and CSN5i-3 on Arabidopsis (Schlierf *et al*., 2016;
317 Altmann *et al*., 2017). In animal cell lines, these inhibitors interfere with the CSN5 deneddylase
318 activity, and trap CRLs in their neddylated states. Because they remain untested on any plant
319 systems, we first determined their efficacy on Col-0 seedlings. Parallel MLN4924 treatments
320 were used as neddylation-inhibition controls. Dose-dependent increments in $CUL1^{Nedd8}$ levels
321 with collateral decrease in unneddylated CUL1 was detected at 24hr post-treatment with
322 CSN5i-3 (Figure 5C). At 48-hrs post-treatment, efficiency of CSN5i-3 inhibitions intensified
323 (Supplemental Figure 7A). At all doses tested, Azaindole#6 remained ineffective in changing
324 $CUL1^{Nedd8}$:CUL1 ratios. As expected, MLN4924 treatments in a dose-dependent manner
325 reduced $CUL1^{Nedd8}$ levels. For subsequent experiments, we continued with 10μM dose of
326 CSN5i-3 and the same for MLN4924, as used in our earlier assays. On Pi-replete Col-0, CSN5i-
327 3 caused a modest increase in basal Pi levels and upregulation in expression of *PHT1;3*, but
328 not significantly for *SPX1* or *IPS1* (Figure 5D-E; Supplemental Figure 7B-C). Under Pi-deplete
329 exposure, CSN5i-3 suppressed the induction of *PHT1;3, SPX1* or *IPS1* in Col-0 and mirrored
330 MLN4924 effects (Figure 5D-E; Supplemental Figure 7B-C). CSN5i-3-treated Col-0 extracts
331 when fractionated, CSN5 was markedly enriched in the CSN holo-complex pools with
332 negligible detection in monomeric elutions, a pattern resembling *ipk1-1*, *itpk1-2,* or Pi-starved
333 profiles (Figure 6A). With these results, we reason strong correlation between CSN5
334 deneddylation deficiencies to its enhanced retention on the CSN holo-complex, and trigger of
335 PSR as observed in *ipk1-1* or *itpk1-2* plants. Most interestingly, *ipk1-1* or *itpk1-2* seedlings
336 grown under sufficient Pi when treated with CSN5i-3 had reduced *IPS1* expressions than
337 untreated plants indicating that skewed kinetics of CSN5 activity rather than its complete
338 inhibition were attributed to these mutants (Supplemental Figure 7D). MLN4924-treatments
339 on *ipk1-1* or *itpk1-2* in Pi-deplete medium offered relief by elevating *IPS1* expressions further

340 supporting our hypothesis that inadequacies in these mutants to support PSR is related to
341 dynamics of CSN5-regulated neddylation/deneddylation cycles of CRLs (Supplemental Figure
342 7E). From these data, it is suggestive that IPK1/ITPK1 functions influence deneddylase
343 efficiencies and shuttling modes of CSN5 thereby affecting CRL requirements in executing
344 PSR.

345 **IP6K1-like activity, but not $InsP_6$ regulates CSN5 deneddylase functions of CSN.**

346 $InsP_6$ is implicated as the physiological glue in potentiating CSN2-CRL associations (Scherer
347 *et al*., 2016). That a kinase-dead IP5K interacts weakly with CSN2/5 further indicates that $InsP_6$
348 augmenting these interactions is produced locally. Supplementing $InsP_6$ to IP5K-depleted cell
349 lysates strengthens CRL-CSN2 associations, and increases deneddylation activities of
350 recombinant CSN on purified neddylated cullins (Scherer *et al*., 2016). Apparently, the
351 externally added metabolite gets access its designated binding pocket at the CRL-CSN2
352 interface. Even though CRL-CSN associations are not affected in *ipk1-1* or *itpk1-2*, we
353 investigated whether adding $InsP_6$ to lysates recover deneddylation deficiencies in these
354 mutants, or augments it in Col-0. In lysate deneddylation assays showed that supplemented
355 $InsP_6$ did not alter deneddylation deficiencies or CUL1 instability in *ipk1-1* or *itpk1-2*
356 (Supplemental Figure 8). In similar assays on Col-0 extracts, $InsP_6$ addition did not change
357 deneddylation or CUL1 turnover rates indicating that unlike mammalian systems, CSN
358 functions in plants are not influenced by $InsP_6$.

359 As a CRL-CSN release factor, $InsP_7$ when supplemented to mammalian cell extracts does not
360 cause complex disassembly meaning that IP6K1 activity is very tightly regulated
361 spatiotemporally (Rao *et al*., 2014). With observed ITPK1-CSN2 interactions, this instigated
362 us to investigate for a similar mechanism in plants. The cell-permeable compound N2-(m-
363 (trifluoromethyl)benzyl) N6-(p-nitrobenzyl) purine (TNP) inhibits animal IP6K1 functions and

364 reduce $InsP_7$ levels (Padmanabhan *et al*., 2009). TNP effects so far have remained untested on
365 Arabidopsis InsPs. In extracts of 10μM TNP-treated Col-0, distinct increase in $CUL1^{NEDD8}$
366 levels were observed although less potent than a similar dose of CSN5i-3 (Figure 6B). To
367 improve TNP efficacies, we used 25μM doses for subsequent assays. In Col-0 grown in Pi-
368 sufficient media, TNP presence replicated CSN5i-3 results in augmenting basal Pi levels,
369 upregulation of *IPS1* or *PHT1;3* expressions, and more retention of CSN5 in the CSN holo-
370 complex pools (Figure 6A-C-D). TNP also suppressed endogenous deneddylation rates with
371 increased CUL1 instability (Figure 6E). And likewise, to CSN5i-3, TNP also suppressed PSI-
372 gene inductions in Col-0 under Pi-deplete circumstances (Figure 6D). Curiously, CSN5i-3,
373 TNP or MLN4924 treatments on *itpk1-2:ITPK1-GFP* resulted in increased ITPK1-GFP levels,
374 similar to observed in Pi-deplete media (Supplemental Figure 9). Although direct inhibitions
375 of TNP on Arabidopsis ITPK1 or other $InsP_{(6)}$-kinases still remains to be tested, nevertheless
376 our results imply that similar to mammals an IP6K1-like activity affects CSN5 performance on
377 regulating CUL1 deneddylation rates and its consequences on PSR. Overall, with our data we
378 present localized coordinated involvement of InsP-kinase pair in modulating CSN dynamics,
379 defining molecular concept of the CSN paradox, and underlining CSN role in phosphate stress
380 responses of plants.

381

382 **Discussion**

383 In animal systems, CRL-CSN tether is augmented by $InsP_6$ and released via stimulus-driven
384 $InsP_7$ synthesis. Here, we show that although Arabidopsis IPK1 and ITPK1 retain conserved
385 CSN interactions, $InsP_6$/$InsP_7$ changes in the corresponding mutants do not overall affect
386 CRL1-CSN associations. Thus, either the residual levels of these InsPs suffice at the CRL-
387 CSN junctures or the association/dissociation cycles involve an altogether different InsP(s) not

388 locally altered in the above mutants. Unlike mammalian results, that added $InsP_6$ does not
389 rescue *ipk1-1* or even alter CUL1 deneddylation rates/stability in Col-0 supports our
390 speculation. Further, an *ITPK4* mutant (*itpk4-1*) with reduced $InsP_6$/$InsP_7$ as in *ipk1-1* or *itpk1-*
391 *2* has normal PSR (Kuo *et al*., 2018) and matches Col-0 ratio of $CUL1^{Nedd8}$:CUL1 also lends
392 credence to our hypothesis. One striking distinction in *ipk1-1* or *itpk1-2* is that these mutants
393 accumulate increased levels of Ins(3,4,5,6)P_4 which neither the *itpk4-1* nor Col-0 subjected to
394 PSR does (Kuo *et al*., 2018). Whether this increased abundance of Ins(3,4,5,6)P_4 or another
395 unidentified InsP altered in *ipk1-1* or *itpk1-2* satisfy CRL-CSN interaction requirements
396 remains a possibility to explore further. Nevertheless, analogous to mammals our observations
397 overall parallel that decreased CSN5 deneddylase performance with lower CUL1
398 deneddylation rates associate with the loss of IPK1 or ITPK1 and implicates their distinct roles
399 on CSN functions.

400 Mammalian ITPK1 over-expression partitions more monomeric CSN5 free from the CSN
401 holo-complex (Sun *et al*., 2002). We demonstrate here that absence of Arabidopsis ITPK1 or
402 TNP inhibitions antagonize CSN5 release from the CSN holo-complex. Even with yet to be
403 tested TNP effects on ITPK1 (or another InsP-kinase) functions in plants, nonetheless a
404 mammalian IP6K1-like activity in choreographing CSN5 entry-exit shuttles seems to be
405 conserved in Arabidopsis. Overall structural integrity of an inert CSN holo-complex is
406 remarkably maintained without CSN5, albeit for deneddylation CSN5 incorporation is
407 mandatory (Lingaraju *et al*., 2014). When CSN5 is integrated into the holo-complex, its
408 interfaces with CSN4-CSN6 inhibit deneddylase activation in the absence of a bound CRL
409 (Enchev *et al*., 2012; Lingaraju *et al*., 2014). Upon binding a neddylated CRL, a series of
410 conformational change prompted by CSN4 orients CSN5 active site towards the neddylated
411 cullins. Closely proximal to this active site, conserved lysines in CSN2 alpha helices coordinate
412 bound $InsP_6$ to bridge for more stable associations with CRL. The bound $InsP_6$ in this

413 electropositive environment is uniquely oriented with its 5'-phosphate exposed, amenable for
414 subsequent pyrophosphorylation. Contrastingly, when an $InsP_7$ is modeled into the same active
415 site strong steric clashes especially at CRL-CSN junctures are noted (Lin *et al*., 2020). These
416 steric intolerances may underlie $InsP_7$-triggered CSN5 deneddylase activation, followed by
417 CRL and perhaps CSN5 release from the CSN holo-complex. When added to cell lysates, since
418 free $InsP_7$ fails to enhance cullin neddylation or disrupt CRL-CSN associations (Rao *et al*.,
419 2014), its localized synthesis achieved through site-specific availability of $InsP_6$, and its
420 accessibility to CSN5 active site is hence crucial for its proposed role. Thus, similar to the
421 mammalian IP6K1 a plant ITPK1 activity (via $InsP_7$ or an unknown InsP) may possess
422 propensity to reconfigure CSN, initiating deneddylation coupled to CRLs and CSN5
423 disassembly from the holo-complex. These roles may be supportive of the recent implication
424 that a plant ITPK1 has evolutionarily integrated functional signatures of both mammalian
425 ITPK1 and IP6K1 (Whitfield *et al*., 2020).

426 With obvious $InsP_8$ reductions in *ipk1-1*, *itpk1-2* or upon VIH2 phosphatase activity during Pi-
427 starvation (Dong *et al*., 2019; Zhu *et al*., 2019), PHR1 liberated from SPX1 causes activation
428 of PSI-gene expressions. Here we demonstrate that a mode of perception of Pi-deprivation in
429 addition to the above also occurs at CSN, involving changes in associated InsP-kinase
430 activities, and is responded by decreased deneddylation rates with pronounced CSN5 retentions
431 on the CSN holo-complex. Since the resulting increase in $CUL1^{Nedd8}$ levels remain independent
432 of PHR1/PHL1 presence, these observations likely indicate parallel responsive routes of a Pi-
433 starved plant to facilitate more available pools of neddylated CRLs to ubiquitinylate substrates
434 including the recently identified SPX4, released from PHR1-hold (Osorio *et al*., 2019). These
435 features we show are constitutive in *ipk1-1*, *itpk1-2*, and mimicked in wild-type plants with
436 CSN5i-3 or TNP treatment, and suppressed by the neddylation inhibitor MLN4924. Our
437 observation that phosphate re-supplementation post-starvation restores CSN5 partitioning and

438 CUL^{Nedd8}:CUL1 ratios to Pi-replete patterns in wild-type plants implies that the noted shifts
439 are only transitory adaptations. That, unlike in *ipk1-1* or *itpk1-2*, global polyubiquitin-
440 conjugates remains unchanged in Col-0 under low-Pi availability additionally emphasize on
441 the strictly regulatory PSR mechanisms to controls ubiquitinylation-specificities on intended
442 targets. Not the least, observed failure in *itpk1-2* (Riemer *et al*., 2020) or *csn5a-2* to respond to
443 low-Pi by anticipated augmentation of already upregulated PSI-gene expressions, or in CSN5i-
444 3 or TNP treated Col-0 indicates that CSN5 partitioning re-adjustments are only shifts in
445 neddylation/deneddylation equilibrium and not a complete inhibition of the CSN5
446 deneddylase. Also, that MLN4924 presence causes sub-optimal induction of PSI-gene
447 expressions in Pi-depleted Col-0, suggests continued requirements of CRL
448 neddylation/deneddylation cycles to successfully transduce PSR. Thus, sustained and
449 successful response to Pi-starvation is likely achieved by a shift in equilibrium of CSN5-
450 mediated deneddylation dynamics on CUL1 and not complete inhibition of its activities as
451 described in our model (Figure 7). Similar phenomenon is mirrored by the shuttling
452 requirements of CSN5 in cell proliferation wherein its perturbations cause complete arrest
453 (Tomoda *et al*., 2002; Yoshida *et al*., 2010).

454 Distinct increase in ITPK1 protein but not gene expression under Pi-starvation (Riemer *et al*.,
455 2020) and as shown here with CSN5i-3, TNP or MLN4924 treatments is conceivably similar
456 to the gain of stability the mammalian IP6K1 acquires upon CRL binding (Rao *et al*., 2014).
457 Thus, similar to CUL1 vulnerability for self-ubiquitinylation, ITPK1 fates may also be
458 regulated in the absence of CRL substrates. Increased stabilities hence may therefore reflect
459 ITPK1's priority to accommodate stimulus-appropriate co-factor requirements in downstream
460 responses not limited only for modulating CRL functions. The mammalian phosphate exporter
461 Xenotropic and polytropic retrovirus receptor 1 (XPR1) relies on $InsP_7$ synthesized by IP6K1/2
462 for function (Wilson *et al*., 2019). Arabidopsis XPR1 ortholog PHO1 does not complement the

463 *pho1* mutant if mutations are introduced in its $InsP_7$-binding pocket (Wild *et al*., 2016). And as
464 is known during PSR, augmented auxin responses involving SCF^{TIR1} also require $InsP_7$ (Laha
465 *et al*., 2020). Whether these new engagements of ITPK1 are adaptation strategies to transiently
466 deprive CSN (and CSN5 release from the holo-complex) and shift balances towards more
467 neddylated CRL availability and/or for providing $InsP_7$ for other cellular processes are
468 encouraging possibility to explore. In conclusion, with our data we highlight remarkable
469 conservation, albeit with slight distinction, in plant InsP-kinase roles in regulating CRL-CSN
470 functions and its implications in responding to Pi-imbalances.

471

472 **References**

473 **Adepoju O, Williams SP, Craige B, Cridland CA, Sharpe AK, Brown AM, Land E, Perera IY,**
474 **Mena D, Sobrado P, Gillaspy GE** (2019) bioRxiv**:**724914; doi:
475 https://doi.org/10.1101/724914
476 **Altmann E, Erbel P, Renatus M, Schaefer M, Schlierf A, Druet A, Kieffer L, Sorge M, Pfister K,**
477 **Hassiepen U, Jones M, Ruedisser S, Ostermeier D, Martoglio B, Jefferson AB,**
478 **Quancard J** (2017) Azaindoles as Zinc-Binding Small-Molecule Inhibitors of the JAMM
479 Protease CSN5. Angew Chem Int Ed Engl **56:** 1294-1297
480 **Bhattacharjee S, Halane MK, Kim SH, Gassmann W** (2011) Pathogen effectors target
481 Arabidopsis EDS1 and alter its interactions with immune regulators. Science **334:** 1405-
482 1408
483 **Bustos R, Castrillo G, Linhares F, Puga MI, Rubio V, Perez-Perez J, Solano R, Leyva A, Paz-**
484 **Ares J** (2010) A central regulatory system largely controls transcriptional activation and
485 repression responses to phosphate starvation in Arabidopsis. PLoS Genet **6:** e1001102
486 **Chakrabarty R, Banerjee R, Chung SM, Farman M, Citovsky V, Hogenhout SA, Tzfira T,**
487 **Goodin M** (2007) pSITE vectors for stable integration or transient expression of
488 autofluorescent protein fusions in plants: probing *Nicotiana benthamiana*-virus
489 interactions. Mol Plant Microbe Interact **20:** 740-750
490 **Chamovitz DA, Segal D** (2001) JAB1/CSN5 and the COP9 signalosome. A complex situation.
491 EMBO Reports **2:** 96-101
492 **Chiou TJ, Aung K, Lin SI, Wu CC, Chiang SF, Su CL** (2006) Regulation of phosphate homeostasis
493 by MicroRNA in Arabidopsis. Plant Cell **18:** 412-421
494 **Cope GA, Suh GS, Aravind L, Schwarz SE, Zipursky SL, Koonin EV, Deshaies RJ** (2002) Role of
495 predicted metalloprotease motif of Jab1/Csn5 in cleavage of Nedd8 from Cul1. Science
496 **298:** 608-611
497 **Desai M, Rangarajan P, Donahue JL, Williams SP, Land ES, Mandal MK, Phillippy BQ, Perera**
498 **IY, Raboy V, Gillaspy GE** (2014) Two inositol hexakisphosphate kinases drive inositol
499 pyrophosphate synthesis in plants. Plant J **80:** 642-653
500 **Dohmann EM, Kuhnle C, Schwechheimer C** (2005) Loss of the CONSTITUTIVE
501 PHOTOMORPHOGENIC9 signalosome subunit 5 is sufficient to cause the cop/det/fus
502 mutant phenotype in Arabidopsis. Plant Cell **17:** 1967-1978

503 **Dohmann EM, Levesque MP, Isono E, Schmid M, Schwechheimer C** (2008) Auxin responses in
504 mutants of the Arabidopsis CONSTITUTIVE PHOTOMORPHOGENIC9 signalosome. Plant
505 Physiol **147:** 1369-1379
506 **Dong J, Ma G, Sui L, Wei M, Satheesh V, Zhang R, Ge S, Li J, Zhang TE, Wittwer C, Jessen HJ,**
507 **Zhang H, An GY, Chao DY, Liu D, Lei M** (2019) Inositol Pyrophosphate $InsP_8$ Acts as an
508 Intracellular Phosphate Signal in Arabidopsis. Mol Plant **12:** 1463-1473
509 **Dubiel D, Rockel B, Naumann M, Dubiel W** (2015) Diversity of COP9 signalosome structures
510 and functional consequences. FEBS Lett **589:** 2507-2513
511 **Dubiel W** (2009) Resolving the CSN and CAND1 paradoxes. Mol Cell **35:** 547-549
512 **Enchev RI, Scott DC, da Fonseca PC, Schreiber A, Monda JK, Schulman BA, Peter M, Morris**
513 **EP** (2012) Structural basis for a reciprocal regulation between SCF and CSN. Cell Rep **2:**
514 616-627
515 **Gillaspy GE** (2013) The role of phosphoinositides and inositol phosphates in plant cell signaling.
516 Adv Exp Med Biol **991:** 141-157
517 **Gusmaroli G, Feng S, Deng XW** (2004) The Arabidopsis CSN5A and CSN5B subunits are present
518 in distinct COP9 signalosome complexes, and mutations in their JAMM domains exhibit
519 differential dominant negative effects on development. Plant Cell **16:** 2984-3001
520 **Hakenjos JP, Richter R, Dohmann EM, Katsiarimpa A, Isono E, Schwechheimer C** (2011)
521 MLN4924 is an efficient inhibitor of NEDD8 conjugation in plants. Plant Physiol **156:** 527-
522 536
523 **Ham BK, Chen J, Yan Y, Lucas WJ** (2018) Insights into plant phosphate sensing and signaling.
524 Curr Opin Biotechnol **49:** 1-9
525 **Huang H, Quint M, Gray WM** (2013) The *eta7/csn3-3* auxin response mutant of Arabidopsis
526 defines a novel function for the CSN3 subunit of the COP9 signalosome. PLoS One **8:**
527 e66578
528 **Jia Q, Kong D, Li Q, Sun S, Song J, Zhu Y, Liang K, Ke Q, Lin W, Huang J** (2019) The Function of
529 Inositol Phosphatases in Plant Tolerance to Abiotic Stress. Int J Mol Sci **20**
530 **Jia X, Chanda B, Zhao M, Brunner AM, Beers EP** (2015) Instability of the Arabidopsis mutant
531 *csn5a-2* caused by epigenetic modification of intronic T-DNA. Plant Sci **238:** 53-63
532 **Jung JY, Ried MK, Hothorn M, Poirier Y** (2018) Control of plant phosphate homeostasis by
533 inositol pyrophosphates and the SPX domain. Curr Opin Biotechnol **49:** 156-162
534 **Kim SH, Gao F, Bhattacharjee S, Adiasor JA, Nam JC, Gassmann W** (2010) The Arabidopsis
535 resistance-like gene SNC1 is activated by mutations in SRFR1 and contributes to
536 resistance to the bacterial effector AvrRps4. PLoS Pathog **6:** e1001172
537 **Kuo HF, Chang TY, Chiang SF, Wang WD, Charng YY, Chiou TJ** (2014) Arabidopsis inositol
538 pentakisphosphate 2-kinase, AtIPK1, is required for growth and modulates phosphate
539 homeostasis at the transcriptional level. Plant J **80:** 503-515
540 **Kuo HF, Hsu YY, Lin WC, Chen KY, Munnik T, Brearley CA, Chiou TJ** (2018) Arabidopsis
541 inositol phosphate kinases IPK1 and ITPK1 constitute a metabolic pathway in
542 maintaining phosphate homeostasis. Plant J **95**:613-630
543 **Laha D, Johnen P, Azevedo C, Dynowski M, Weiss M, Capolicchio S, Mao H, Iven T,**
544 **Steenbergen M, Freyer M, Gaugler P, de Campos MK, Zheng N, Feussner I, Jessen HJ,**
545 **Van Wees SC, Saiardi A, Schaaf G** (2015) VIH2 Regulates the Synthesis of Inositol
546 Pyrophosphate $InsP_8$ and Jasmonate-Dependent Defenses in Arabidopsis. Plant Cell **27:**
547 1082-1097
548 **Laha D, Parvin N, Hofer A, Giehl RFH, Fernandez-Rebollo N, von Wiren N, Saiardi A, Jessen**
549 **HJ, Schaaf G** (2019) Arabidopsis ITPK1 and ITPK2 Have an Evolutionarily Conserved
550 Phytic Acid Kinase Activity. ACS Chem Biol **14:** 2127-2133
551 **Laha NP, Dhir YW, Giehl RFH, Schäfer EM, Gaugler P, Shishavan ZH, Gulabani H, Mao H,**
552 **Zheng N, von Wirén N, Jessen HJ, Saiardi A, Bhattacharjee S, Laha D, Schaaf G** (2020)
553 bioRxiv: 2020.04.23.058487
554 **Lee HS, Lee DH, Cho HK, Kim SH, Auh JH, Pai HS** (2015) $InsP_6$-sensitive variants of the Gle1
555 mRNA export factor rescue growth and fertility defects of the *ipk1* low-phytic-acid
556 mutation in Arabidopsis. Plant Cell **27:** 417-431

557 **Lin H, Zhang X, Liu L, Fu Q, Zang C, Ding Y, Su Y, Xu Z, He S, Yang X, Wei X, Mao H, Cui Y, Wei**
558 **Y, Zhou C, Du L, Huang N, Zheng N, Wang T, Rao F** (2020) Basis for metabolite-
559 dependent Cullin-RING ligase deneddylation by the COP9 signalosome. Proc Natl Acad Sci
560 U S A **117:** 4117-4124
561 **Lingaraju GM, Bunker RD, Cavadini S, Hess D, Hassiepen U, Renatus M, Fischer ES, Thoma**
562 **NH** (2014) Crystal structure of the human COP9 signalosome. Nature **512:** 161-165
563 **Lv Q, Zhong Y, Wang Y, Wang Z, Zhang L, Shi J, Wu Z, Liu Y, Mao C, Yi K, Wu P** (2014) SPX4
564 Negatively Regulates Phosphate Signaling and Homeostasis through Its Interaction with
565 PHR2 in Rice. Plant Cell **26:** 1586-1597
566 **Monserrate JP, York JD** (2010) Inositol phosphate synthesis and the nuclear processes they
567 affect. Curr Opin Cell Biol **22:** 365-373
568 **Mosadeghi R, Reichermeier KM, Winkler M, Schreiber A, Reitsma JM, Zhang Y, Stengel F,**
569 **Cao J, Kim M, Sweredoski MJ, Hess S, Leitner A, Aebersold R, Peter M, Deshaies RJ,**
570 **Enchev RI** (2016) Structural and kinetic analysis of the COP9-Signalosome activation and
571 the cullin-RING ubiquitin ligase deneddylation cycle. Elife **5:** e12102
572 **Murphy AM, Otto B, Brearley CA, Carr JP, Hanke DE** (2008) A role for inositol
573 hexakisphosphate in the maintenance of basal resistance to plant pathogens. Plant J **56:**
574 638-652
575 **Osorio MB, Ng S, Berkowitz O, De Clercq I, Mao C, Shou H, Whelan J, Jost R** (2019) SPX4 Acts
576 on PHR1-Dependent and -Independent Regulation of Shoot Phosphorus Status in
577 Arabidopsis. Plant Physiol **181:** 332-352
578 **Padmanabhan U, Dollins DE, Fridy PC, York JD, Downes CP** (2009) Characterization of a
579 selective inhibitor of inositol hexakisphosphate kinases: use in defining biological roles
580 and metabolic relationships of inositol pyrophosphates. J Biol Chem **284:** 10571-10582
581 **Puga MI, Mateos I, Charukesi R, Wang Z, Franco-Zorrilla JM, de Lorenzo L, Irigoyen ML,**
582 **Masiero S, Bustos R, Rodriguez J, Leyva A, Rubio V, Sommer H, Paz-Ares J** (2014)
583 SPX1 is a phosphate-dependent inhibitor of Phosphate Starvation Response 1 in
584 Arabidopsis. Proc Natl Acad Sci U S A **111:** 14947-14952
585 **Qin ZX, Chen QJ, Tong Z, Wang XC** (2005) The Arabidopsis inositol 1,3,4-trisphosphate 5/6
586 kinase, AtItpk-1, is involved in plant photomorphogenesis under red light conditions,
587 possibly via interaction with COP9 signalosome. **43:** 947-954
588 **Rao F, Xu J, Khan AB, Gadalla MM, Cha JY, Xu R, Tyagi R, Dang Y, Chakraborty A, Snyder SH**
589 (2014) Inositol hexakisphosphate kinase-1 mediates assembly/disassembly of the CRL4-
590 signalosome complex to regulate DNA repair and cell death. Proc Natl Acad Sci U S A **111:**
591 16005-16010
592 **Ried MK, Wild R, Zhu J, Broger L, Harmel RK, Hothorn LA, Fiedler D, Hothorn M** (2019)
593 Inositol pyrophosphates promote the interaction of SPX domains with the coiled-coil
594 motif of PHR transcription factors to regulate plant phosphate homeostasis. bioRxiv
595 2019.12.13.875393
596 **Riemer E, Laha D, Harmel RK, Gaugler P, Pries V, Frei M, Hajirezaei M-R, Laha NP,**
597 **Krusenbaum L, Schneider R, Jessen HJ, Saiardi A, Fiedler D, Schaaf G, Giehl RFH**
598 (2020) ITPK1 is an $InsP_6$/ADP phosphotransferase that controls systemic phosphate
599 homeostasis in Arabidopsis. bioRxiv 2020.05.18.100297
600 **Ruan W, Guo M, Wang X, Guo Z, Xu Z, Xu L, Zhao H, Sun H, Yan C, Yi K** (2019) Two RING-Finger
601 Ubiquitin E3 Ligases Regulate the Degradation of SPX4, An Internal Phosphate Sensor, for
602 Phosphate Homeostasis and Signaling in Rice. Mol Plant **12:** 1060-1074
603 **Rubio V, Linhares F, Solano R, Martin AC, Iglesias J, Leyva A, Paz-Ares J** (2001) A conserved
604 MYB transcription factor involved in phosphate starvation signaling both in vascular
605 plants and in unicellular algae. Genes Dev **15:** 2122-2133
606 **Scherer PC, Ding Y, Liu Z, Xu J, Mao H, Barrow JC, Wei N, Zheng N, Snyder SH, Rao F** (2016)
607 Inositol hexakisphosphate (IP6) generated by IP5K mediates cullin-COP9 signalosome
608 interactions and CRL function. Proc Natl Acad Sci U S A **113:** 3503-3508
609 **Schlierf A, Altmann E, Quancard J, Jefferson AB, Assenberg R, Renatus M, Jones M,**
610 **Hassiepen U, Schaefer M, Kiffe M, Weiss A, Wiesmann C, Sedrani R, Eder J, Martoglio**

611 **B** (2016) Targeted inhibition of the COP9 signalosome for treatment of cancer. Nat
612 Commun **7:** 13166
613 **Sheard LB, Tan X, Mao H, Withers J, Ben-Nissan G, Hinds TR, Kobayashi Y, Hsu FF, Sharon**
614 **M, Browse J, He SY, Rizo J, Howe GA, Zheng N** (2010) Jasmonate perception by inositol-
615 phosphate-potentiated COI1-JAZ co-receptor. Nature **468:** 400-405
616 **Shears SB, Ganapathi SB, Gokhale NA, Schenk TM, Wang H, Weaver JD, Zaremba A, Zhou Y**
617 (2012) Defining signal transduction by inositol phosphates. Subcell Biochem **59:** 389-412
618 **Shears SB, Wang H** (2019) Inositol phosphate kinases: Expanding the biological significance of
619 the universal core of the protein kinase fold. Adv Biol Regul **71:** 118-127
620 **Soucy TA, Smith PG, Milhollen MA, Berger AJ, Gavin JM, Adhikari S, Brownell JE, Burke KE,**
621 **Cardin DP, Critchley S, Cullis CA, Doucette A, Garnsey JJ, Gaulin JL, Gershman RE,**
622 **Lublinsky AR, McDonald A, Mizutani H, Narayanan U, Olhava EJ, Peluso S, Rezaei M,**
623 **Sintchak MD, Talreja T, Thomas MP, Traore T, Vyskocil S, Weatherhead GS, Yu J,**
624 **Zhang J, Dick LR, Claiborne CF, Rolfe M, Bolen JB, Langston SP** (2009) An inhibitor of
625 NEDD8-activating enzyme as a new approach to treat cancer. Nature **458:** 732-736
626 **Stevenson-Paulik J, Bastidas RJ, Chiou ST, Frye RA, York JD** (2005) Generation of phytate-free
627 seeds in Arabidopsis through disruption of inositol polyphosphate kinases. Proc Natl
628 Acad Sci U S A **102:** 12612-12617
629 **Sun Y, Wilson MP, Majerus PW** (2002) Inositol 1,3,4-trisphosphate 5/6-kinase associates with
630 the COP9 signalosome by binding to CSN1. J Biol Chem **277:** 45759-45764
631 **Szijgyarto Z, Garedew A, Azevedo C, Saiardi A** (2011) Influence of inositol pyrophosphates on
632 cellular energy dynamics. Science **334:** 802-805
633 **Tan X, Calderon-Villalobos LI, Sharon M, Zheng C, Robinson CV, Estelle M, Zheng N** (2007)
634 Mechanism of auxin perception by the TIR1 ubiquitin ligase. Nature **446:** 640-645
635 **Tomoda K, Kubota Y, Arata Y, Mori S, Maeda M, Tanaka T, Yoshida M, Yoneda-Kato N, Kato**
636 **JY** (2002) The cytoplasmic shuttling and subsequent degradation of $p27^{Kip1}$ mediated by
637 Jab1/CSN5 and the COP9 signalosome complex. J Biol Chem **277:** 2302-2310
638 **Whitfield H, White G, Sprigg C, Riley AM, Potter BVL, Hemmings AM, Brearley CA** (2020) An
639 ATP-responsive metabolic cassette comprised of inositol tris/tetrakisphosphate kinase 1
640 (ITPK1) and inositol pentakisphosphate 2-kinase (IPK1) buffers diphosphosphoinositol
641 phosphate levels. Biochem J **477:** 2621-2638
642 **Wild R, Gerasimaite R, Jung JY, Truffault V, Pavlovic I, Schmidt A, Saiardi A, Jessen HJ,**
643 **Poirier Y, Hothorn M, Mayer A** (2016) Control of eukaryotic phosphate homeostasis by
644 inositol polyphosphate sensor domains. Science **352:** 986-990
645 **Williams SP, Gillaspy GE, Perera IY** (2015) Biosynthesis and possible functions of inositol
646 pyrophosphates in plants. Front Plant Sci **6:** 67
647 **Wilson MS, Jessen HJ, Saiardi A** (2019) The inositol hexakisphosphate kinases IP6K1 and -2
648 regulate human cellular phosphate homeostasis, including XPR1-mediated phosphate
649 export. J Biol Chem **294:** 11597-11608
650 **Wundenberg T, Mayr GW** (2012) Synthesis and biological actions of diphosphoinositol
651 phosphates (inositol pyrophosphates), regulators of cell homeostasis. Biol Chem **393:**
652 979-998
653 **Yi Sun WW, Jianping Jin** (2020) CRL Book Sun et al 2020. Advances in Experimental Medicine
654 and Biology Biology and Therapeutics **1217**
655 **Yoshida A, Yoneda-Kato N, Panattoni M, Pardi R, Kato JY** (2010) CSN5/Jab1 controls multiple
656 events in the mammalian cell cycle. FEBS Lett **584:** 4545-4552
657 **Zhong Y, Wang Y, Guo J, Zhu X, Shi J, He Q, Liu Y, Wu Y, Zhang L, Lv Q, Mao C** (2018) Rice SPX6
658 negatively regulates the phosphate starvation response through suppression of the
659 transcription factor PHR2. **219:** 135-148
660 **Zhu J, Lau K, Puschmann R, Harmel RK, Zhang Y, Pries V, Gaugler P, Broger L, Dutta AK,**
661 **Jessen HJ, Schaaf G, Fernie AR, Hothorn LA, Fiedler D, Hothorn M** (2019) Two
662 bifunctional inositol pyrophosphate kinases/phosphatases control plant phosphate
663 homeostasis. Elife **8:** e43582

664 **Figure legends**

665 **Fig. 1. IPK1 and ITPK1 interact with each other and with selective CSN or CRLs**
666 **components *in planta*.** *(A)* Immuno-enrichments of IPK1 *(top panel)* or ITPK1 *(bottom panel)*
667 from corresponding complemented lines (*ipk1-1:Myc-IPK1* or *itpk1-2:ITPK1-GFP*,
668 respectively) was probed with anti-CSN1/2/4/5, anti-CUL1, or anti-ASK1 antibodies. IgG-
669 agarose enrichments were used as negative controls. *(B)* Bimolecular Fluorescence
670 Complementation (BiFC) assays showing *in planta* IPK1 or ITPK1 interaction with CSN1/2
671 and with each other. Indicated binary vectors combinations were co-expressed via
672 Agrobacterium in *Nicotiana benthamiana* leaves and fluorescence observed under a confocal
673 microscope with YFP filter. Scale bar=50 µm. *(C)* Co-immunoprecipitation of transiently
674 expressed GFP-ITPK1 with Myc-IPK1 from *N. benthamiana* leaves. Anti-GFP pulldown was
675 probed with anti-GFP or anti-Myc antibodies.

676 **Fig. 2. CSN5 deneddylase deficiencies with increased holo-complex retention in *ipk1-1* or**
677 ***itpk1-2* cause enhanced CUL1^{Nedd8} levels.** *(A)* IPK1 or ITPK1 does not co-elute with the CSN
678 holo-complex. *(B)* Enhanced CSN5 engagements on the CSN holo-complex in *ipk1-1* and
679 *itpk1-2*. Extracts from marked plants fractionated by size-exclusion chromatography were
680 immuno-blotted with indicated antibodies. Fraction numbers and elution positions of molecular
681 weight standards (in kDa) are shown. Fractions corresponding to CSN holo-complex and CSN
682 subunit monomeric elutions are marked. *(C)* Immuno-enrichment of CUL1 detects
683 stoichiometrically similar amounts of CSN1 and CSN2 in *ipk1-1* or *itpk1-2* to Col-0. Pulldowns
684 with either IgG or anti-CUL1 antibodies were probed with anti-CUL1, anti-CSN1 or anti-
685 CSN2 antibodies. *(D)* Increased CUL1^{Nedd8} levels (*top panel*) and enhanced global
686 polyubiquitin-conjugates (*bottom panel*) in *ipk1-1* or *itpk1-2*. Total protein extracts were
687 probed with anti-CUL1, anti-actin, or anti-Ubiquitin antibodies as indicated. *(E)* CSN5-
688 deneddylation deficiencies and lower CUL1 half-life in *ipk1-1* or *itpk1-2*. In-lysate CUL1

689 deneddylation assay (Lin *et al*., 2020) at the indicated time points (minutes post-incubation;
690 mpi) probed with anti-CUL1 antibodies. Migration position of molecular weight standards (in
691 kDa) and neddylated ($CUL1^{Nedd8}$) or unneddylated (CUL1) Cullin1 are shown. Anti-actin or
692 Ponceau S staining demonstrates loadings controls.

693 **Fig. 3. Enhanced $CUL1^{Nedd8}$ levels associated with PSR is essential for PSI-gene**
694 **inductions.** MLN4924 suppresses *(A)* elevated PSI-gene expressions, and *(B)* higher
695 endogenous Pi-levels in *ipk1-1* or *itpk1-2*. *(C)* Induction of *PHT1;3* or *IPS1* expressions in Col-
696 0 upon Pi-starvation is inhibited by MLN4924. *(D)* Increments in $CUL1^{Nedd8}$ levels during Pi-
697 deprivation is PHR1/PHL1-independent. Plants grown in Pi-replete medium or transferred to
698 Pi-deplete medium were treated with or without MLN4924. Gene expression changes were
699 relative to *MON1* transcripts and reported as fold-change to Col-0 levels. Data is mean $\pm$ SD
700 (n=3 for qPCRs; n=6-7 for Pi-estimations). Statistical significance indicated with different
701 alphabets is according to post-hoc Tukey's test ($p<0.05$). For *PHT1;3* or *SPX1* expression data,
702 statistical comparisons were to their respective DMSO-treated Col-0. For immunoblots, anti-
703 CUL1 antibodies were used. Ponceau S staining shows loadings controls.

704 **Fig. 4. Pi-starvation reduces endogenous CSN5 deneddylase activity and is restored upon**
705 **phosphate resupply.** *(A)* Extracts at indicated time points (minutes post-incubation; mpi) from
706 in-lysate CUL1 deneddylation assay on Col-0 from Pi-replete or Pi-deplete media were probed
707 with anti-CUL1 antibodies. *(B)* Restoration of enhanced $CUL1^{Nedd8}$ levels occur upon Pi-
708 resupply post-starvation. *(C)* Increased retention of CSN5 on the CSN holo-complex under Pi-
709 deplete exposure is reversed with Pi-resupply. *(D)* Global levels of polyubiquitin-conjugates
710 remain unchanged during PSR. For these assays, plants were subjected to Pi-starvation for 3
711 days and phosphate re-supplementation was done for 12hrs. Comparable loadings are shown
712 by Ponceau S staining. Elution positions of molecular weight standards (in kDa) are indicated.

713 **Fig. 5. Inhibition of CSN5 functions activates PSR under Pi-replete but confers non-**
714 **responsiveness under Pi-deplete growth.** *csn5a-2* plants have *(A)* elevated endogenous Pi
715 levels, *(B)* increased *PHT1;3* or *SPX1* transcript levels under Pi-replete growth but suppressed
716 expression upon Pi-starvation. *(C)* CSN5i-3 inhibits Arabidopsis CUL1 deneddylation, *(D)*
717 elevates endogenous Pi-levels, and *(E)* suppresses *PHT1;3* induction during phosphate-
718 deprivation. Immunoblots were probed with anti-CUL1 antibodies. Ponceau S staining shows
719 loading controls. Inhibitor treatments were done for 24 hrs and doses used are indicated.
720 Expression levels of *MON1* transcripts was used as an internal reference for qPCRs and
721 reported as fold-change relative to DMSO-treated Col-0 under Pi-replete growth. Error bars
722 are mean $\pm$ SD (n=3 for qPCRs; n=6-7 for Pi-estimations). Different alphabets denote statistical
723 significance determined by post-hoc Tukey's test ($p<0.05$). *PHT1;3* and *SPX1* data are
724 compared to respective Pi-replete Col-0.

725 **Fig. 6. CSN5i-3 or TNP treatments on Col-0 mirrors *ipk1-1* or *itpk1-2* properties.** *(A)*
726 CSN5 partition shifts to CSN holo-complex pools upon CSN5i-3 or TNP treatment. TNP *(B)*
727 enhances pools of $CUL1^{Nedd8}$, *(C)* increases endogenous Pi-content, *(D)* upregulates *IPS1* or
728 *PHT1;3* expressions under Pi-replete, but suppresses them under Pi-deplete growth, and *(E)*
729 decreases endogenous deneddylation rates with increased CUL1 instability. Immunoblots were
730 probed with anti-CUL1 or anti-CSN5 antibodies as indicated. Ponceau S staining shows
731 loading controls. Expression levels of *MON1* transcripts was used as internal reference for
732 qPCRs. Error bars are mean $\pm$ SD (n=3 for qPCRs; n=6-7 for Pi-estimations). Statistical
733 significance according post-hoc Tukey's test ($p<0.05$) is shown with different alphabets.

734 **Fig. 7. Schematic representation of CRL-CSN dynamics in plants.** CSN holo-complex
735 platform protects CRLs in the absence of bound ubiquitinylation substrate (steric hindrance
736 prevents E2 enzyme binding (Enchev *et al*., 2012; Mosadeghi *et al*., 2016) utilizing coordinated
737 activities (bi-directional white arrows) of the IPK1-ITPK1 pair. Equilibrium is maintained

738 between CSN-mediated deneddylation cycles and $CUL1^{Nedd8}$ requirements in steady-state CRL
739 functions. Balanced assembly/disassembly cycles of CSN5 on the CSN holo-complex are also
740 linked to these regulations. Perception (via unknown mode; question mark) of a stimulus, such
741 as Pi-starvation, reduces CSN5 deneddylase functions, likely via more facilitation of the InsP-
742 kinase functions to CRL-SCF complex roles in targeted ubiquitinylation (Ub^n) and degradation
743 of specific substrates (such as SPX4 or Aux/IAAs). IPK1-ITPK1 pair provides necessary InsP
744 co-factors to these activities. Inhibition modes of TNP, CSN5i-3 and MLN4924 are indicated
745 at the respective processes. CSN subunits are presented as numbers; CUL1, Cullin1; RBX,
746 RING H2 protein1; E2, Ubiquitin cojugating enzyme E2; SA, substrate adapter; SR, substrate
747 receptor; N8, Nedd8; IPK1, Inositol pentakisphosphate 2-kinase1; ITPK1, Inositol 1,3,4-
748 trisphosphate 5/6-kinase 1.

749

750 **Materials and Methods**

751 **Plant material and growth conditions.** Details of *Arabidopsis thaliana* (ecotype Col-0) T-
752 DNA insertion lines *ipk1-1, itpk1-2, ipk2β-1*, *itpk4-1*, *csn5a-2*, *vih2-4, itpk1-2:ITPK1-GFP,*
753 and *phr1 phl1* plants have been described earlier (Kuo *et al*., 2014; Jia *et al*., 2015; Kuo *et al*.,
754 2018; Laha *et al*., 2020). T-DNA and respective gene-specific primers are listed in
755 Supplementary Table 1. Seeds were stratified for 2-days at 4^oC in dark and then sterilized using
756 30% bleach solution. They were then germinated either directly on soil or on ½ strength
757 Murashige and Skoog (MS) Pi-replete (625 μM KH_2PO_4) agar plates in growth chambers
758 maintained at 22^oC with 70% Relative humidity (RH) and 16hrs: 8hrs; light: dark having light
759 intensity 100 μmol $\mu m^{-2}s^{-1}$. For fractionation, Pi-starvation assays, and inhibitor treatments,
760 plants grown on media plates as above were transferred 7-days post-germination to liquid ½
761 MS medium in 12-well sterile culture plates are proceeded accordingly as indicated in

762 respective experiments. For immuno-precipitation assays 4-week-old soil-grown plants were
763 used.

764 **Size-exclusion chromatography of plant extracts.** Gel-filtration protocol was according to
765 Huang *et al* (2013). Briefly, 14-day-old plants ground to a fine powder with liquid nitrogen
766 were homogenized in Gel filtration buffer (50mM Tris-HCl pH 7.5, 150mM NaCl, 1mM
767 EDTA, 10% Glycerol, 10mM $MgCl_2$, 1mM DTT, 1mM PMSF and 1X Protease inhibitor
768 cocktail). Homogenates were centrifuged for 10 mins at 4^oC and supernatant passed through
769 0.2 μM syringe filters. Total protein extracts were fractionated through Superdex 10/300 GL
770 Column (GE- Healthcare, USA) and eluted in the fractionation buffer at 0.2mL/min flow rate.
771 The eluants were TCA (Trichloroacetic acid) precipitated, washed with acetone and
772 resuspended in 1X Laemmli loading dye and used for indicated immunoblots.

773 **In-lysate deneddylation assay.** In-lysate deneddylayion assay was according to Lin *et al*
774 (2020). Briefly, 14-day-old seedlings were quickly homogenized in deneddylayion buffer
775 (10mM Tris-HCl pH7.5, 150mM NaCl and 0.5% NP-40) in absence of protease inhibitors. The
776 extracts were incubated at 37^oC for indicated times, reaction stopped by adding Laemmli
777 loading dye to 1X, and then used for immunoblots.

778 **Phosphate-starvation/re-supplementation assays.** After germination of seeds as described
779 earlier, seedlings were transferred to liquid ½ MS medium in 12-well sterile culture plates with
780 Pi-replete conditions (625 μM KH_2PO_4) and placed in the growth chamber. After 4-days, the
781 plants were either maintained with Pi-replete or transferred to Pi-deplete (10 μM KH_2PO_4)
782 liquid media and continued for another 3 days (total 14-days post-germination) before being
783 used for Pi-estimation, qRT-PCR, total protein extraction, or fractionation assays. For Pi-
784 resupply, plants in Pi-deplete medium were transferred to Pi-replete medium for 12 hrs before
785 analysis.

786 **Inhibitor treatments.** Stock solutions of MLN4924 (Cayman Chemicals, USA), CSN5i-3
787 (Novartis Inc, Switzerland), or TNP (Sigma-Aldrich, USA) was prepared in DMSO. For
788 treatments, 10µM final concentration of MLN4924 or CSN5i-3 were used. TNP was used at
789 25µM final unless otherwise indicated. For assays on Col-0, *ipk1-1*, or *itpk1-2* or for
790 fractionations, inhibitors were treated for 24hrs. For effects on PSR, inhibitors were added
791 during the shift to Pi-deplete medium.

792 **Ubiquitination assays.** For determining global ubiquitination levels, extracts from indicated
793 plants prepared in Gel filtration buffer in the presence of 10µM proteasome inhibitor MG132
794 were incubated on ice for 2hrs. Immunoblotting was then performed with anti-ubiquitin
795 antibodies (P4D1; SantaCruz Biotechnology, USA).

796 **Statistical analysis.** All Data presented here are representative of at least three biological and
797 technical replicates for each. Post-hoc Tukey's test ($p<0.05$) were applied for statistical
798 analysis.

799 Additional details of cloning methodologies for generation of constructs, and transgenic lines,
800 BiFC assays, immuno-enrichments, immunoblotting, Pi-estimations, and qRT-PCRs are
801 described in *Supplementary Materials and Methods*.

802

803 **Acknowledgements**

804 We thank Regional Centre for Biotechnology (RCB), Faridabad, for financial support, lab
805 infrastructure, and central instrumental facilities. S.B. expresses gratitude to Department of
806 Biotechnology (DBT), Govt. of India for the award of Ramalingaswami re-entry fellowship
807 and Grant (No. BT/PR23666/AGIII/103/1039/2018) that supported this research. The *phr1*
808 *phl1* double mutant seeds were from Prof. Tzyy-Jen Chiou, Academia Sinica, Taipei. A special

809 thanks to Dr. Eva Altmann, Novartis Institutes for BioMedical Research, Switzerland for the
810 CSN5i-3 gift. Also to Dr. Divya Chandran (RCB) for help with transcriptomic data analysis of
811 *csn* mutants. Y.W. thanks DBT for Young Investigator award. M.K. and K.D.I thank UGC and
812 DBT for fellowships, respectively. D.L. acknowledges the Indian Institute of Science for start-
813 up funds. All authors thanks Dr. Nripendra Singh and his team at Advanced Technology
814 Platform Centre (ATPC), Faridabad, India for constant support with sample fractionations.

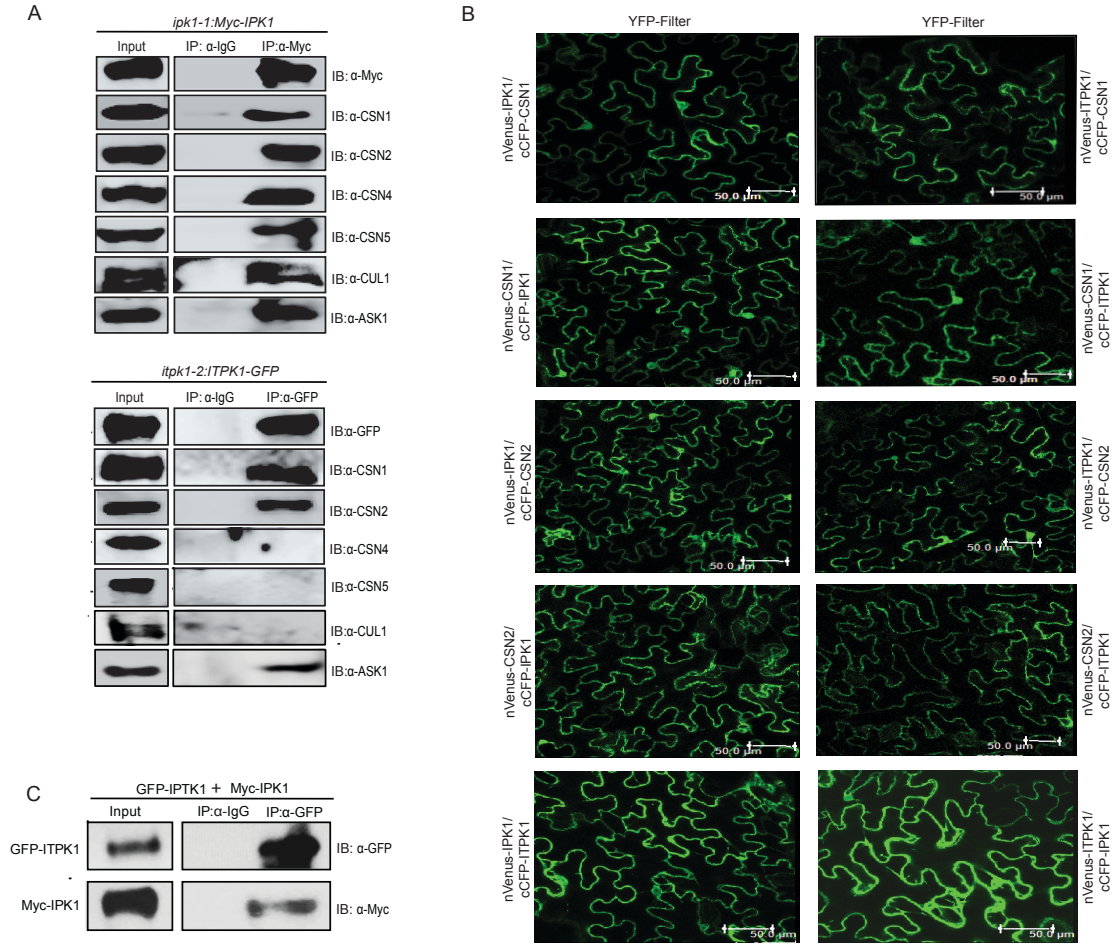

Fig. 1. IPK1 and ITPK1 interact with each other and with selective CSN or CRLs components *in planta*. *(A)* Immuno-enrichments of IPK1 *(top panel)* or ITPK1 *(bottom panel)* from corresponding complemented lines (*ipk1-1:Myc-IPK1* or *itpk1-2:ITPK1-GFP*, respectively) was probed with anti-CSN1/2/4/5, anti-CUL1, or anti-ASK1 antibodies. IgG-agarose enrichments were used as negative controls. *(B)* Bimolecular Fluorescence Complementation (BiFC) assays showing *in planta* IPK1 or ITPK1 interaction with CSN1/2 and with each other. Indicated binary vectors combinations were co-expressed via Agrobacterium in *Nicotiana benthamiana* leaves and fluorescence observed under a confocal microscope with YFP filter. Scale bar=50 µm. *(C)* Co-immunoprecipitation of transiently expressed GFP-ITPK1 with Myc-IPK1 from *N. benthamiana* leaves. Anti-GFP pulldown was probed with anti-GFP or anti-Myc antibodies.

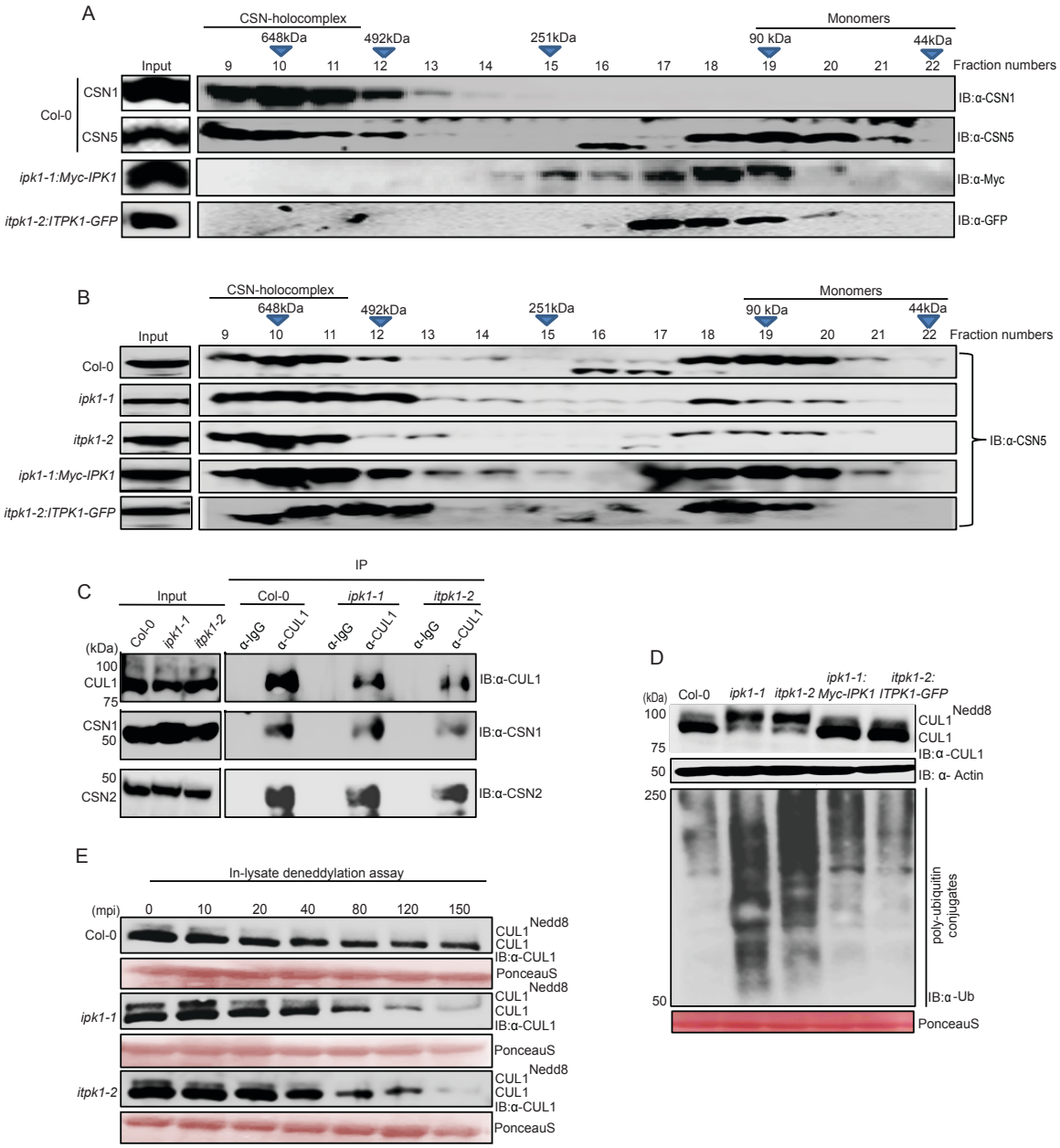

827

828 **Fig. 2. CSN5 deneddylase deficiencies with increased holo-complex retention in *ipk1-1* or**
829 ***itpk1-2* cause enhanced CUL1^{Nedd8} levels.** *(A)* IPK1 or ITPK1 does not co-elute with the CSN
830 holo-complex. *(B)* Enhanced CSN5 engagements on the CSN holo-complex in *ipk1-1* and
831 *itpk1-2*. Extracts from marked plants fractionated by size-exclusion chromatography were
832 immuno-blotted with indicated antibodies. Fraction numbers and elution positions of molecular
833 weight standards (in kDa) are shown. Fractions corresponding to CSN holo-complex and CSN
834 subunit monomeric elutions are marked. *(C)* Immuno-enrichment of CUL1 detects
835 stoichiometrically similar amounts of CSN1 and CSN2 in *ipk1-1* or *itpk1-2* to Col-0. Pulldowns
836 with either IgG or anti-CUL1 antibodies were probed with anti-CUL1, anti-CSN1 or anti-
837 CSN2 antibodies. *(D)* Increased CUL1^{Nedd8} levels (*top panel*) and enhanced global
838 polyubiquitin-conjugates (*bottom panel*) in *ipk1-1* or *itpk1-2*. Total protein extracts were
839 probed with anti-CUL1, anti-actin, or anti-Ubiquitin antibodies as indicated. *(E)* CSN5-
840 deneddylation deficiencies and lower CUL1 half-life in *ipk1-1* or *itpk1-2*. In-lysate CUL1

841 deneddylation assay (Lin *et al*., 2020) at the indicated time points (minutes post-incubation;
842 mpi) probed with anti-CUL1 antibodies. Migration position of molecular weight standards (in
843 kDa) and neddylated ($CUL1^{Nedd8}$) or unneddylated (CUL1) Cullin1 are shown. Anti-actin or
844 Ponceau S staining demonstrates loadings controls. Migration position of molecular weight
845 standards (in kDa) and neddylated ($CUL1^{Nedd8}$) or unneddylated (CUL1) cullin1 are shown.
846 Anti-actin or Ponceau S staining demonstrate loadings controls.

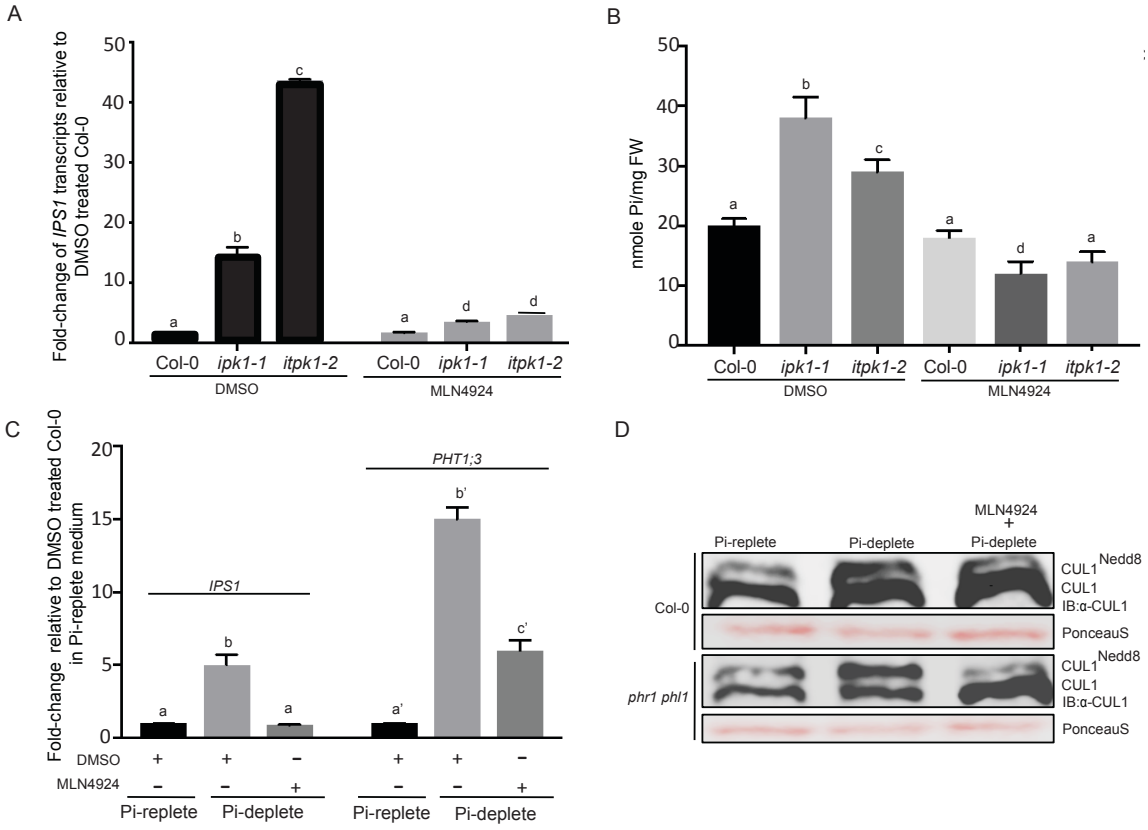

847

848 **Fig. 3. Enhanced CUL1^{Nedd8} levels associated with PSR is essential for PSI-gene**
849 **inductions.** MLN4924 suppresses *(A)* elevated PSI-gene expressions, and *(B)* higher
850 endogenous Pi-levels in *ipk1-1* or *itpk1-2*. *(C)* Induction of *PHT1;3* or *IPS1* expressions in Col-
851 0 upon Pi-starvation is inhibited by MLN4924. *(D)* Increments in CUL1^{Nedd8} levels during Pi-
852 deprivation is PHR1/PHL1-independent. Plants grown in Pi-replete medium or transferred to
853 Pi-deplete medium were treated with or without MLN4924. Gene expression changes were
854 relative to *MON1* transcripts and reported as fold-change to Col-0 levels. Data is mean $\pm$ SD
855 (n=3 for qPCRs; n=6-7 for Pi-estimations). Statistical significance indicated with different
856 alphabets is according to post-hoc Tukey's test ($p<0.05$). For *PHT1;3* or *SPX1* expression data,
857 statistical comparisons were to respective DMSO-treated Col-0. For immunoblots, anti-CUL1
858 antibodies were used. Ponceau S staining shows loadings controls.

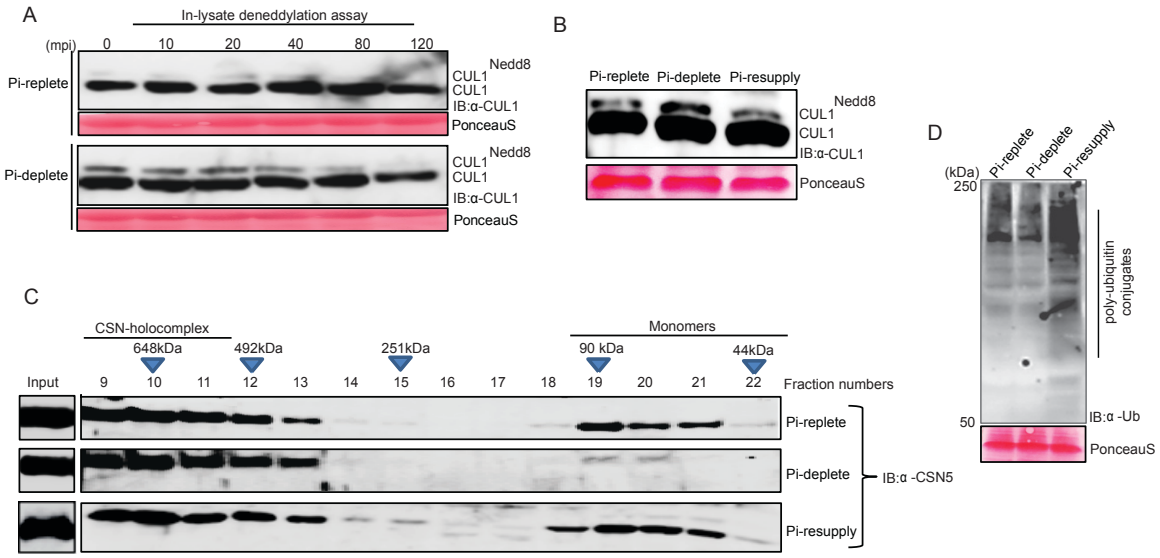

Fig. 4. Pi-starvation reduces endogenous CSN5 deneddylase activity and is restored upon phosphate resupply. *(A)* Extracts at indicated time points (minutes post-incubation; mpi) from in-lysate CUL1 deneddylation assay on Col-0 from Pi-replete or Pi-deplete media were probed with anti-CUL1 antibodies. *(B)* Restoration of enhanced $CUL1^{Nedd8}$ levels occur upon Pi-resupply post-starvation. *(C)* Increased retention of CSN5 on the CSN holo-complex under Pi-deplete exposure is reversed with Pi-resupply. *(D)* Global levels of polyubiquitin-conjugates remain unchanged during PSR. For these assays, plants were subjected to Pi-starvation for 3 days and phosphate re-supplementation was done for 12hrs. Comparable loadings are shown by Ponceau S staining. Elution positions of molecular weight standards (in kDa) are indicated.

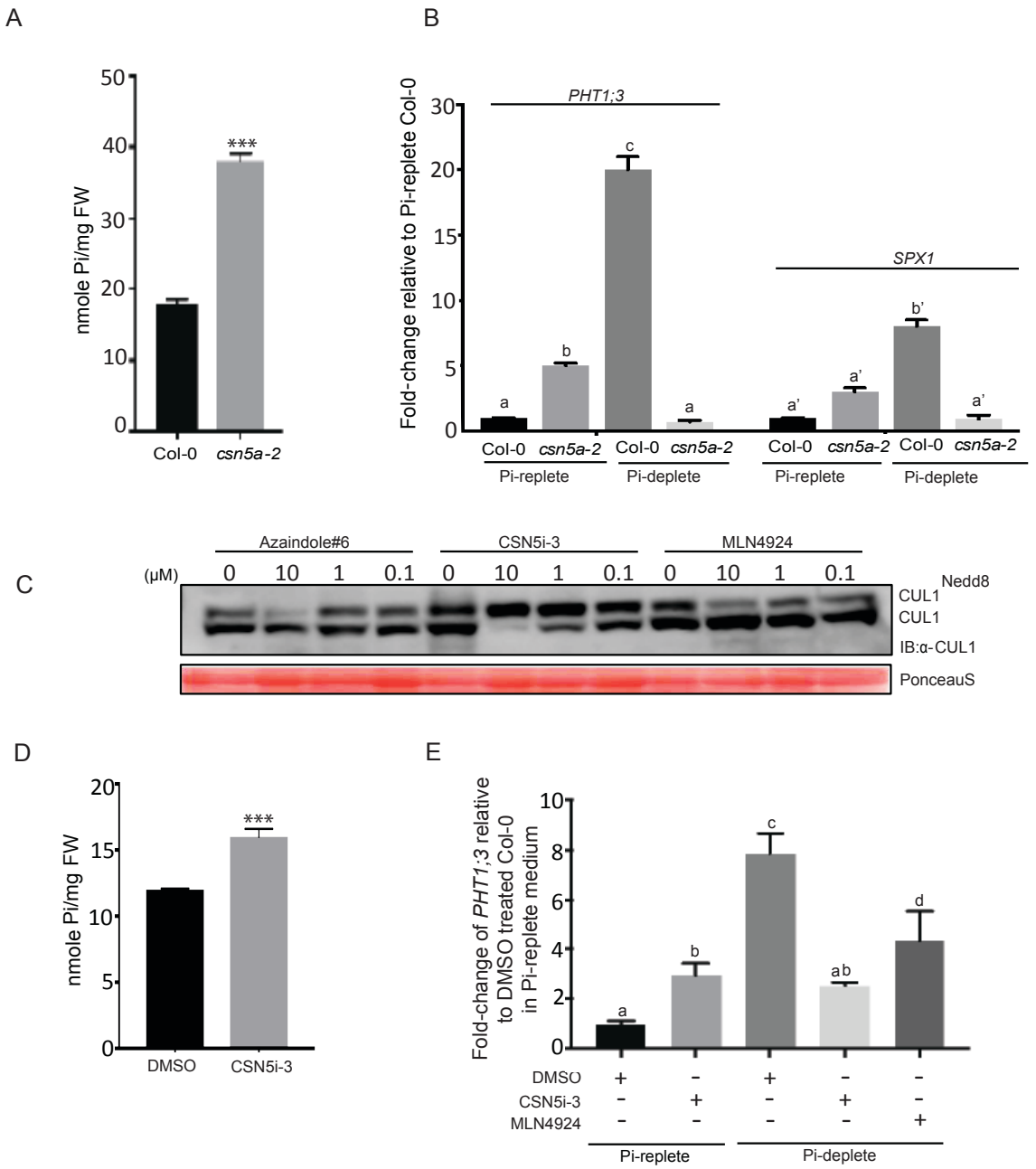

Fig. 5. Inhibition of CSN5 functions activates PSR under Pi-replete but confers non-responsiveness under Pi-deplete growth. *csn5a-2* plants have *(A)* elevated endogenous Pi levels, *(B)* increased *PHT1;3* or *SPX1* transcript levels under Pi-replete growth but suppressed expression upon Pi-starvation. *(C)* CSN5i-3 inhibits Arabidopsis CUL1 deneddylation, *(D)* elevates endogenous Pi-levels, and *(E)* suppresses *PHT1;3* induction during phosphate-deprivation. Immunoblots were probed with anti-CUL1 antibodies. Ponceau S staining shows loading controls. Inhibitor treatments were done for 24 hrs and doses used are indicated. Expression levels of *MON1* transcripts was used as an internal reference for qPCRs and reported as fold-change relative to DMSO-treated Col-0 under Pi-replete growth. Error bars are mean ± SD (n=3 for qPCRs; n=6-7 for Pi-estimations). Different alphabets denote statistical significance determined by post-hoc Tukey's test ($p<0.05$). *PHT1;3* and *SPX1* data are compared to respective Pi-replete Col-0.

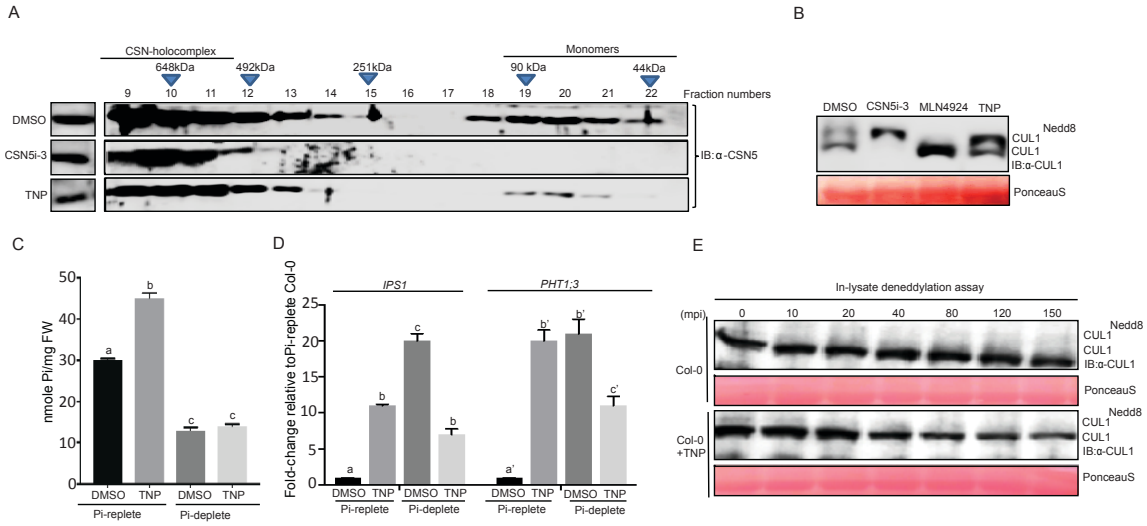

Fig. 6. CSN5i-3 or TNP treatments on Col-0 mirrors *ipk1-1* or *itpk1-2* properties. *(A)* CSN5 partition shifts to CSN holo-complex pools upon CSN5i-3 or TNP treatment. TNP *(B)* enhances pools of $CUL1^{Nedd8}$, *(C)* increases endogenous Pi-content, *(D)* upregulates *IPS1* or *PHT1;3* expressions under Pi-replete, but suppresses them under Pi-deplete growth, and *(E)* decreases endogenous deneddylation rates with increased CUL1 instability. Immunoblots were probed with anti-CUL1 or anti-CSN5 antibodies as indicated. Ponceau S staining shows loading controls. Expression levels of *MON1* transcripts was used as internal reference for qPCRs. Error bars are mean $\pm$ SD (n=3 for qPCRs; n=6-7 for Pi-estimations). Statistical significance according post-hoc Tukey's test ($p<0.05$) is shown with different alphabets.

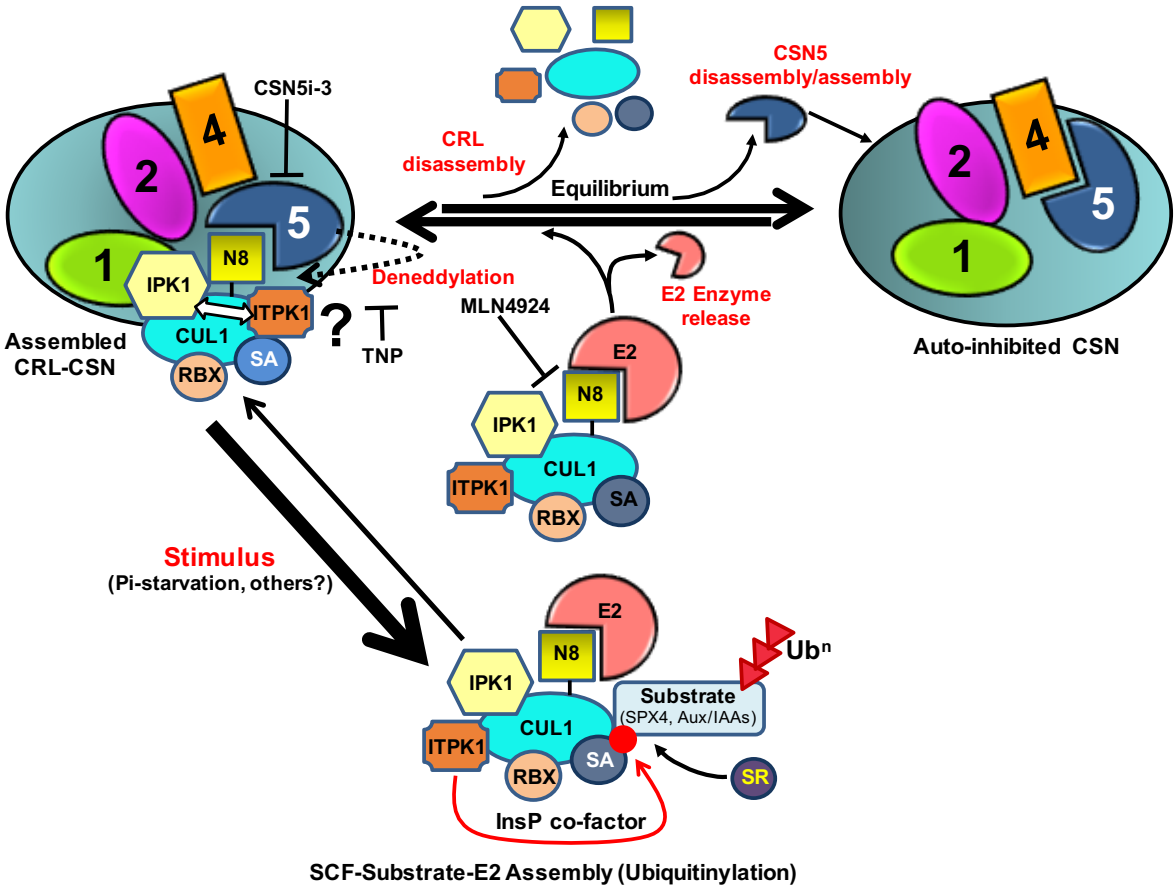

892

893 **Fig. 7. Schematic representation of CRL-CSN dynamics in plants.** CSN holo-complex
894 platform protects CRLs in the absence of bound ubiquitinylation substrate (steric hindrance
895 prevents E2 enzyme binding (Enchev *et al*., 2012; Mosadeghi *et al*., 2016) utilizing coordinated
896 activities (bi-directional white arrows) of the IPK1-ITPK1 pair. Equilibrium is maintained
897 between CSN-mediated deneddylation cycles and $CUL1^{Nedd8}$ requirements in steady-state CRL
898 functions. Balanced assembly/disassembly cycles of CSN5 on the CSN holo-complex are also
899 linked to these regulations. Perception (via unknown mode; question mark) of a stimulus, such
900 as Pi-starvation, reduces CSN5 deneddylase functions, likely via more facilitation of the InsP-
901 kinase functions to CRL-SCF complex roles in targeted ubiquitinylation (Ub^n) and degradation
902 of specific substrates (such as SPX4 or Aux/IAAs). IPK1-ITPK1 pair provides necessary InsP
903 co-factors to these activities. Inhibition modes of TNP, CSN5i-3 and MLN4924 are indicated
904 at the respective processes. CSN subunits are presented as numbers; CUL1, Cullin1; RBX,
905 RING H2 protein1; E2, Ubiquitin cojugating enzyme E2; SA, substrate adapter; SR, substrate
906 receptor; N8, Nedd8; IPK1, Inositol pentakisphosphate 2-kinase1; ITPK1, Inositol 1,3,4-
907 trisphosphate 5/6-kinase 1.